BRNO UNIVERSITY OF TECHNOLOGY
VYSOKÉ UČENÍ TECHNICKÉ V BRNĚ

FACULTY OF CHEMISTRY
FAKULTA CHEMICKÁ

INSTITUTE OF MATERIALS SCIENCE
ÚSTAV CHEMIE MATERIÁLŮ

THE EFFECT OF ORGANIC AND INORGANIC ADDITIVES ON THE CHEMICO-PHYSICAL PROPERTIES OF BIOPOLYMER SUBSTRATES FOR TISSUE ENGINEERING

VLIV ORGANICKÝCH I ANORGANICKÝCH ADITIV NA CHEMICKO-FYZIKÁLNÍ VLASTNOSTI BIOPOLYMERNÍCH SUBSTRÁTŮ PRO TKÁŇOVÉ INŽENÝRSTVÍ

BACHELOR'S THESIS
BAKALÁŘSKÁ PRÁCE

AUTHOR
AUTOR PRÁCE
Martin Kohoutek

SUPERVISOR
VEDOUCÍ PRÁCE
Ing. Jana Brtníková, Ph.D.

BRNO 2020

BRNO UNIVERSITY OF TECHNOLOGY
FACULTY OF CHEMISTRY

Specification Bachelor's Thesis

Project no.:	FCH-BAK1473/2019	Academic year:	2019/20
Department:	Institute of Materials Science		
Student:	**Martin Kohoutek**		
Study programme:	Chemistry and Chemical Technologies		
Study branch:	Chemistry, Technology and Properties of Materials		
Head of thesis:	**Ing. Jana Brtníková, Ph.D.**		

Title of Bachelor's Thesis:

The effect of organic and inorganic additives on the chemico–physical properties of biopolymer substrates for tissue engineering

Bachelor's Thesis:

1) Literary research on the influence of additions of organic and inorganic additives on chemical and physical properties of biopolymer substrates intended for applications in tissue engineering.
2) Preparation of biopolymer substrates with addition of organic and inorganic additives.
3) Monitoring of the effect of addition of both organic and inorganic additives on physico–chemical properties of biopolymer substrates.
4) Evaluation of results and their discussion.
5) Conclusion.

Deadline for Bachelor's Thesis delivery: 31.7.2020:

Bachelor's Thesis should be submitted to the institute's secretariat in a number of copies as set by the dean This specification is part of Bachelor's Thesis

Martin Kohoutek Student	Ing. Jana Brtníková, Ph.D. Head of thesis	doc. Ing. František Šoukal, Ph.D. Head of department
		prof. Ing. Martin Weiter, Ph.D. Dean

In Brno dated 31.1.2020

ABSTRACT

This bachelor's thesis deals with the preparation and characterization of composite collagenous scaffolds for possible applications in both bone and skin tissue engineering with an emphasis on their chemico-physical properties. In the theoretical part, the selected components for fabrication of the scaffolds are described and later were used to fabricate 3D porous composite scaffolds in the experimental part.

Altogether, four different composite collagenous scaffold types and a reference pure collagen scaffold type were prepared using the freeze-drying fabrication technique. Two scaffold types were made by combining collagen with either oxidised cellulose (OC) or carboxymethyl cellulose (CMC). The other two types of scaffolds had the same biopolymeric origin enhanced with the addition of bioceramics based on the hydroxyapatite and tricalcium phosphates.

The microstructure, porosity and pore size were assessed by the scanning electron microscopy. The highest porosity and pore size were achieved by the reference purely collagenous scaffolds, followed by the collagen composites with OC and CMC. Scaffolds with the content of bioceramics had the lowest porosity and pore size, especially those containing CMC. Swelling behaviour analysis and enzymatic degradation *in vitro* showed, that the hydrophilicity and mass loss in the degradation process correlate with each other. The scaffolds without bioceramics were more hydrophilic and achieved greater mass loss than the scaffolds containing bioceramics. The pure collagen was in the between the two groups. Scaffolds containing CMC achieved greater mass loss and hydrophilicity than their OC counterparts. In terms of mechanical properties, scaffolds with bioceramics achieved higher compressive strength in the wet state than the other three scaffold types. The mechanical properties were generally better for scaffolds with lower porosity and lower hydrophilicity.

KEYWORDS

Composite porous scaffolds, collagen, oxidised cellulose, carboxymethyl cellulose, hydroxyapatite, tricalcium phosphate, tissue engineering, enzymatic degradation, porosity.

ABSTRAKT

Tato bakalářská práce se zabývá přípravou a charakterizací kompozitních kolagenových nosičů, s důrazem na jejich chemicko-fyzikální vlastnosti pro možné aplikace jak v tkáňovém inženýrství kostí, tak i kůže. V teoretické části jsou popsány vybrané komponenty pro přípravu tkáňových nosičů, které byly později použity k přípravě 3D porézních vzorků v experimentální části.

Celkem byly připraveny čtyři typy kompozitních nosičů a jeden referenční typ z čistého kolagenu za použití techniky lyofilizace. Dva typy vzorků sestávaly z kombinace kolagenu a oxidované celulózy (OC) nebo kolagenu a karboxymethyl celulózy (CMC). Další dva typy byly založeny na stejné kombinaci jak předchozí dva typy (kolagen s deriváty celulózy) navíc s přídavkem biokeramiky na bázi hydroxyapatitu a fosforečnanu vápenatého.

Mikrostruktura, porozita a velikost pórů byly vyhodnoceny pomocí skenovací elektronové mikroskopie. Nejvyšší porozity a velikosti pórů dosáhly referenční skafoldy s čistým kolagenem, další v pořadí pak byly kompozity kolagenu s OC a CMC. Nejnižší porozitu a velikost pórů měly skafoldy s biokeramikou, zejména pak ty obsahující i CMC. Při analýze botnání a enzymatické degradaci *in vitro* bylo zjištěno, že hydrofilita a úbytek hmotnosti vzorků v procesu degradace spolu korelují. Nosiče bez biokeramiky byly hydrofilnější a dosáhly větší ztráty hmotnosti než vzorky s biokeramikou. Čistý kolagen byl svými výsledky mezi těmito dvěma skupinami. Vzorky s CMC byly hydrofilnější a degradabilnější než jejich protějšky obsahující OC. Co se týká mechanických vlastností, skafoldy s biokeramikou dosáhly vyšší pevnosti v tlaku v mokrém stavu než skafoldy bez biokeramiky. Mechanické vlastnosti byly obecně lepší u vzorků se snižující se porozitou a hydrofilitou.

.

KLÍČOVÁ SLOVA

Kompozitní porézní nosiče, kolagen, oxidovaná celulóza, karboxymethyl celulóza, hydroxyapatit, fosforečnan vápenatý, tkáňové inženýrství, enzymatická degradace, porozita.

KOHOUTEK, M. *The effect of organic and inorganic additives on the chemico-physical properties of biopolymer substrates for tissue engineering.* Brno: Brno University of Technology, Faculty of Chemistry, 2020. 47 p. Supervisor Ing. Jana Brtníková Ph.D.

DECLARATION

I declare that the bachelor thesis has been worked out by myself and that all the quotations from the used literary sources are accurate and complete. The content of the diploma thesis is the property of the Faculty of Chemistry of Brno University of Technology and all commercial uses are allowed only if approved by both the supervisor and the dean of the Faculty of Chemistry, BUT.

…….
student´s signature

Acknowledgements

I would like to thank my supervisor Ing. Jana Brtníková Ph.D. for the organisation, constructive advices and corrections concerning the thesis and my thesis consultant Ing. Katarína Kacvinská for the help with experimental part and advices during the experiments. I would also like to express my appreciation to doc. Ing. Lucy Vojtová Ph.D. and her team for the opportunity to write this thesis and carry out the research regarding its topic. I wish to acknowledge Ing. Petr Poláček Ph.D. for the instructions regarding the operation with the rheometer for conducting dynamic mechanical analysis and Ing. Kristýna Valová for providing the SEM images. Finally, I would like to thank my family for the continuous support and encouragement which helped me tremendously in the process of writing this thesis.

TABLE OF CONTENTS

1 INTRODUCTION

Tissues and organs have the function to repair themselves when they sustain damage. Their autoregenerating abilities, however, are limited and do not suffice when they suffer a more severe damage to their structure. Therefore, a surgery must take place. Transplanting tissue and organ substitutes from other individual have proven to be a satisfactory solution. However, the availability of the substitutes is poor due to the number of patients exceeding the number of donors. Artificial transplants could be also used, but they cannot replace the living organs to the full extent of their functions.

These limitations gave rise to the emergence of an interdisciplinary field of tissue engineering. Though tissue engineering is still in its developmental stage, it shows great promise in the area of tissue regeneration. It allows to develop fully functional tissue and organ substitutes by processing biomaterials into three-dimensional (3D) structures and using them as a suitable environment for living cells which can create the new tissue. Tissue engineering would ensure availability of the substitutes and replacement of the tissue in all its functions, but it still requires more research to be done. The tissue formation is extremely complex and requires an excellent knowledge of the composition and function of individual tissues in order to be implemented in common applications.

The 3D structures used for tissue mimicking are called scaffolds. Scaffolds have a porous internal microstructure which can mimic the features of the extracellular matrix and act as its substitution in the new tissue creation. They support the living cells in the tissue formation process which is why they are desired in tissue engineering. Scaffolds are fabricated from biomaterials, which include natural polymers, synthetic polymers and bioceramics. The most commonly used natural polymer in tissue engineering is collagen, which has excellent biological but poor mechanical properties. The properties of collagen can be enhanced by making composite scaffolds. The cellulose derivatives (oxidised cellulose, carboxymethyl cellulose) and bioceramics (hydroxyapatite, α and β-tricalcium phosphates) have proven to be adequate components for making composite collagenous scaffolds for skin and bone tissue engineering. This thesis describes the characteristics of these substances and how their combinations influence the end properties of the composite scaffolds.

2 CURRENT STATE OF ART

2.1 Tissue Engineering

Tissue engineering (TE) is a field of science which adopts the knowledge of engineering, life and material sciences and mathematical modelling [1, 2]. Its aim is development of functional tissue and organ substitutes that maintain, restore or enhance function of the tissue that has been injured or is entirely missing [3]. TE uses biomaterials to surpass the body's limited ability to autoregenerate its damaged tissues.

The common approach to achieve the new tissue creation dwells in cultivation of multipotent cells *ex vivo*, seeding them into a three-dimensional (3D) biodegradable matrix and transplantation of the matrix into the body's damaged areas. This biomaterial-cell complex provides the appropriate environment for the growth of the new cells and tissue regeneration while maintaining its architecture and integrity [4]. The success of new tissue creation in TE immensely relies on individual properties as well as the interactions (as shown in *Figure 1*) between three main components: living cells, biomaterial matrix and regulatory signals. These are also called the tissue engineering triad [5].

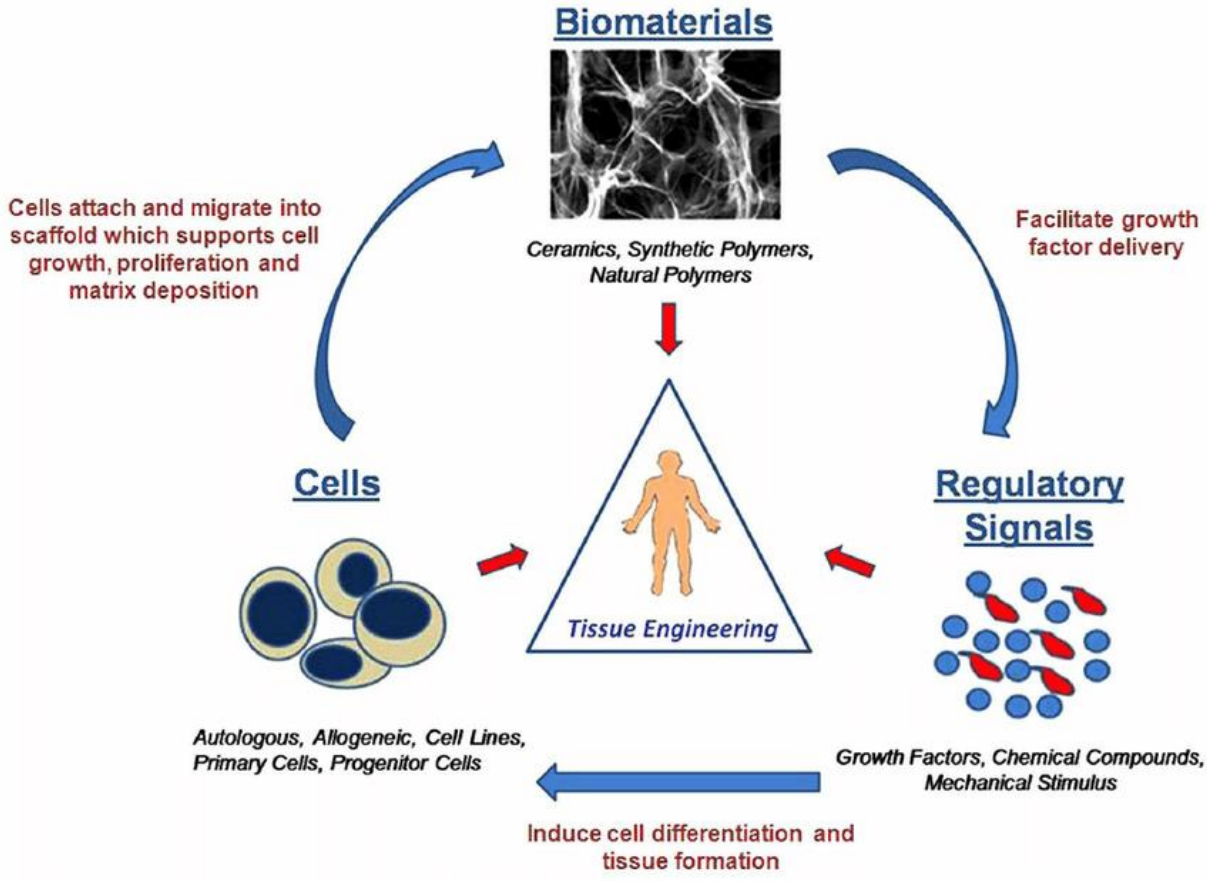

Figure 1 – The components making up tissue engineering triad and connections between them – The delivery of growth factors (signalling molecules) is eased by the 3D structure of biomaterials, Growth factors induce cellular migration, adhesion, proliferation and differentiation to form a tissue, Cells migrate into scaffold pores, adhere to the matrix and proliferate [5].

Biomaterials' role in tissue engineering is to form a scaffold which simulates the extracellular matrix (ECM) before it reforms in the damaged tissue. Two important factors must be taken into account when designing a scaffold: biocompatibility and biodegradability. Biocompatibility refers to aiding tissue formation without causing adverse antigenic and immunogenic response, which could compromise the patient's health. Biodegradability represents dematerialisation of the scaffold's structure after a certain time period, so it does not concur with the newly formed tissue. This also means there is no need for additional surgery to remove it from the affected area. Biomaterials employed in TE are mainly natural polymers, bioceramics and synthetic biodegradable polymers such as PLA or PGA [5].

2.2 Tissue Composition

Knowing the individual tissue components and understanding the interplay between them plays an important role when designing a suitable material for tissue regeneration. Materials used in TE are chosen according to the tissue composition. Since this thesis is focused on tissue engineering of skin and bones, these two tissue types are described in more detail in the following chapters.

2.2.1 Extracellular Matrix

The Extracellular matrix (ECM) is a cell-surrounding structure of a non-cellular character which is present across all tissues and organs. The ECM is created and helped to assemble by the cells themselves. The cells do not cancel their communication with the ECM after its formation and connect to its surface via matrix receptors (e. g. integrins or syndecans) in non-covalent interactions (as in *Figure 2*) [6, 7].

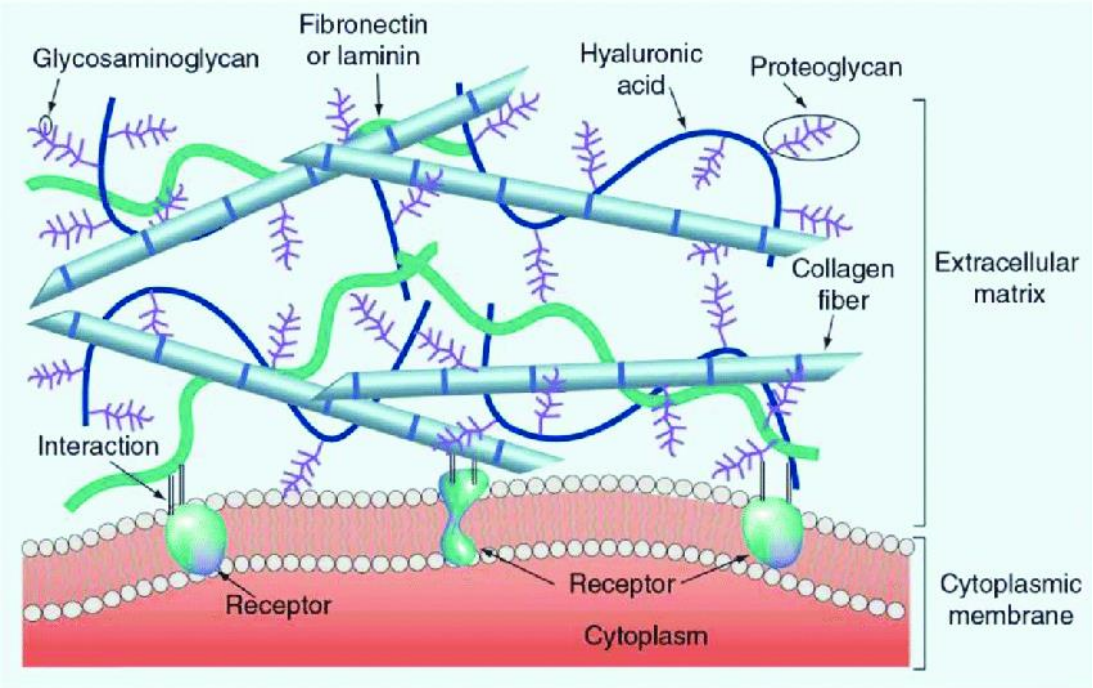

Figure 2 – Extracellular matrix interacting with the cell's surface [8].

Apart from being a physical support for cells, the ECM directly affects tissue morphogenesis and cell differentiation by triggering biochemical and biophysical signals. It binds growth factors which can then interact with the receptors on the cells‘ surface, initiating a signal to regulate gene transcription. The extracellular matrix, thanks to the divergence in its producers, is differs in its composition and properties not only from tissue to tissue, but in some specific cases even in within a single tissue. In the progression of time, it undergoes enzymatic and non-enzymatic remodelling processes that directly impact biochemical and biomechanical properties of the given tissue or organ.

If we unimagine the molecules that pass through the matrix in order to interact with cells, the ECM structure comprises two types of macromolecules: fibrous proteins and proteoglycans. The latter mentioned are macromolecules of high complexity consisting of a core protein and glycosaminoglycan chains. These chains are polymers of disaccharide units which are substituted with amino and carboxy or sulphate ester groups. Proteoglycans contribute to ECM with their influence on hydration which plays a role in binding growth factors.

Being the most abundant fibrous protein of the ECM, collagen has a structural role as well as numerous physiological and developmental functions. It provides tensile strength, is responsible for cell adhesion to the matrix, aids chemotaxis and cell migration and is to a certain extent promoting differentiation. Elastin, which conjoins with collagen, is responsible for ECM resiliency, providing recoil to stretching tissue thanks to its high crosslinking. The last important member of the ECM fibrous protein family is fibronectin with its ability to control ECM organisation and mediate cell attachment by its integrin-binding sites [6, 7].

2.2.2 Skin Structure

Accounting for 15–20 % of a human adult’s body mass, the skin is the largest organ. It serves as a protective barrier, shielding our body insides from surrounding environment, UV radiation, microorganisms and agents of biological, chemical or physical character [9]. Furthermore, the skin helps to regulate body temperature, prevents dehydration, controls substance exchange between the body and its surroundings, generates immune responses and is one of the sensory systems that ensures perception of the outer world [9, 10].

The skin is divided into three layers: epidermis, dermis and hypodermis. The outer layer, epidermis, consists of 4 further layers. Epidermis is formed mostly by keratinocytes, which are born in the innermost layer by differentiation from stem cells [9]. Keratinocytes progress to the epidermis surface and keratinisation gradually occurs, i.e. the cells flatten, lose their organelles including the nucleus and transform into corneocytes with high keratin content. The corneocytes, cells of the outermost epidermis layer, secrete lipids (mostly aramids, cholesterol and free fatty acids) through their lamellar bodies, which are also formed during the keratinisation. This results in a lipid enriched ECM, which plays an essential role in the barrier function of this layer [10].

The second skin layer is the dermis, the thickest layer of the skin, which is attached to epidermis via basal lamina (collagen IV, VII and laminins). It functions as a nutritional and structural support, provides elasticity and strength to the skin and mediates biochemical signalling to the epidermis. The largest dermal cell population are the fibroblasts which produce

fibrillar collagen (mainly types I and III). Other elements of the dermis include immune cells, hair follicles, sweat and sebaceous glands, blood vessels or nerve networks.

The third layer, called the hypodermis, is formed of adipocytes and serves to store subcutaneous fat for energy, heat and mechanical protection purposes. It also contains lymphatic and blood vessels that are larger in size [9, 10]. Other than that, collagen and elastin fibres are also present [11]. All three skin layers and the elements running through them are depicted in *Figure 3*.

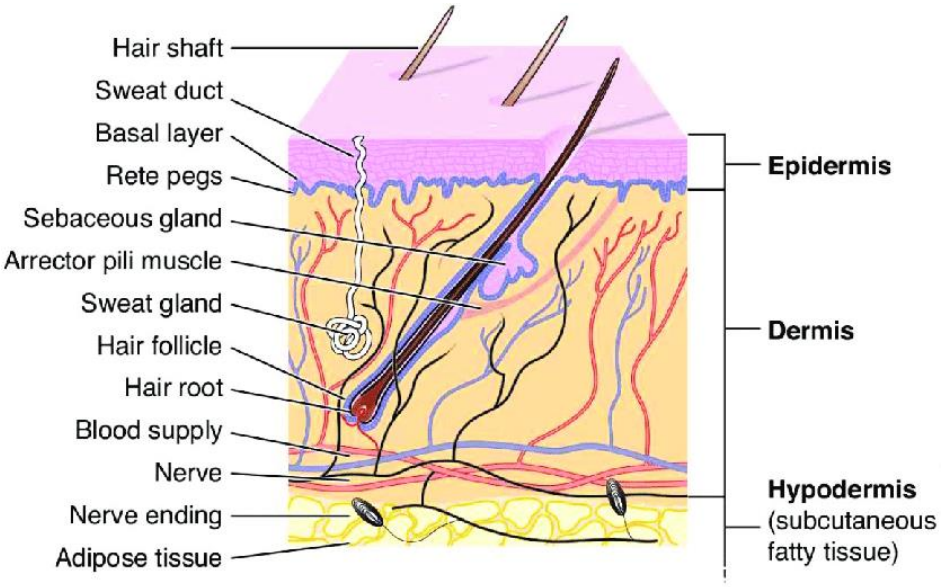

Figure 3 – The layers of the skin and their components [8].

2.2.3 Bone Structure

Bones, as parts of human skeleton, carry several significant functions in the body. While mechanical support for the body and movement of muscles may seem as the primary purposes, bones also protect the internal organs, form the blood cells and maintain mineral and pH homeostasis [12, 13]. Every bone is constantly remodelled, regenerated and repaired due to the damage caused by the repeated stress and aging [14]. Although the shape, structure and function vary across the bone types, what all bones have in common is that they form mineralised collagen fibrils. These are a part of what is called the bone extracellular matrix [15].

The bone ECM contains collagen (predominantly type I with traces of types III and IV), a fibrous protein that makes more than 85 % of the protein present in the bone. The remaining protein of non-collagenous character involves serum albumin, α2-HS-glycoprotein or growth factors to name a few. The bone extracellular matrix stiffness is ensured by mineralization. Bone minerals form 50 to 70 % of the bone weight. The most abundant bone mineral is hydroxyapatite [$Ca_{10}(PO_4)_6(OH)_2$], which occurs in very small crystals with the broadest dimension averaging 200 Å. The small size of crystals helps in mineral metabolism thanks to their better solubility.

Mineralisation is crucial for the bone's strength and mechanical stiffness, with the minerals filling the empty spaces in between the collagen fibrils which provide the elastic resistance. The

mineralisation is aided by the non-collagenous proteins that promote nucleation of crystals, bind to their surfaces and determine their size, shape and quantity.

There are two bone types from the point of the structure: cortical and trabecular bone. Cortical bone is dense, with porosity lesser than 5 % and makes around 80 % of an adult's skeleton. It forms the outer shell of the bone and is thinner around trabecular bone. Trabecular bone forms honeycomb-like network of plates and fibres which are intersecting with the bone marrow. Both bone types, despite taking different shapes, constitute of osteons – a formation of concentric lamellae of the mineralised collagen fibrils. Osteons have circular cross section in cortical bone (broken down in *Figure 4*) and semilunar cross section in trabecular bone [13].

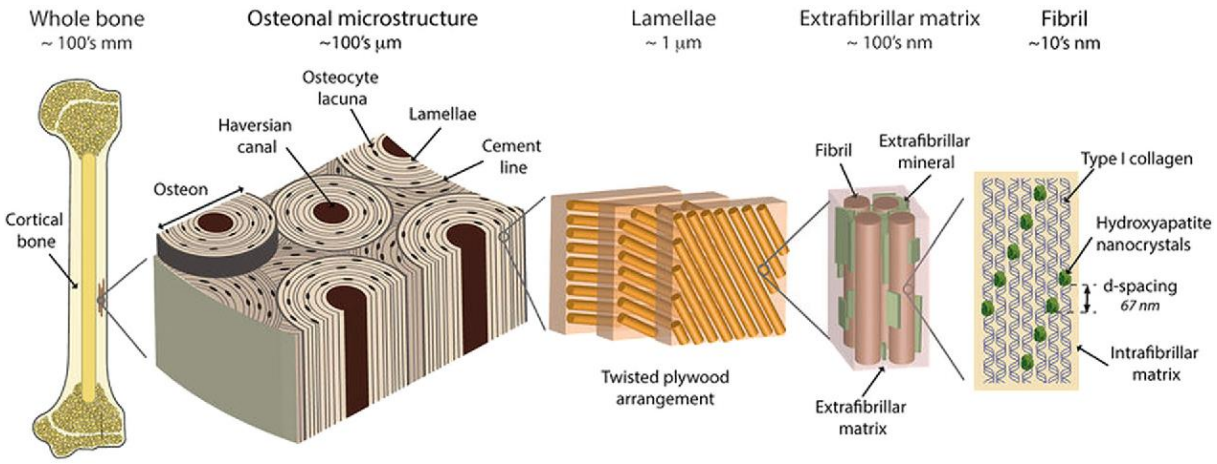

Figure 4 – The hierarchy of cortical bone. Collagen fibrils mineralised with hydroxyapatite assemble into lamellae that arrange concentrically into osteons [16].

2.3 Scaffolds

Role of biomaterial scaffolds was briefly described in the chapter 2.1. They are needed to simulate natural environment of the ECM to provide cells with appropriate mechanical support and encourage their biological function. Cells need to adhere to scaffold's inner surface in order to differentiate and proliferate. This is possible only for scaffolds with a defined pore structure and size.

A scaffold needs to have pore size with a range that corresponds with the cell size. When the pores are too small, cells cannot migrate easily through the scaffold. On the other hand, larger pores take away too much of the surface area and by that also the necessary binding sites for cell adhesion. For effective cell migration and nutrient transport, the pores of a scaffold also must be highly interconnected. The pore size range of scaffolds for skin and bone tissue engineering are noted in *Table 1*. To achieve better mechanical properties of the resulting tissue, it is preferable to have a uniform pore structure in the scaffold [17, 18].

Table 1 – Skin and bone scaffold pore size range [17]

Repaired Tissue	Pore size range (µm)
Skin	20-150
Bone	100-500

Another important parameter of a scaffold is its biodegradability. The proliferating cells residing in the scaffold create their own ECM which, over time, replaces the artificial one. The balance between the rate of new ECM deposition and scaffold degradation should be approximately the same. The degradation occurs either enzymatically or through resorption (depending on the used material) and its rate is hidden in the scaffold's design.

Apart from pore architecture and biodegradability, there are several other properties that must be considered when choosing the material to create a scaffold from. These include biocompatibility, non-toxicity of the scaffold's degradation products, presence of cell binding sites and enough mechanical integrity to remain in the desired shape. The biomaterials used for scaffold fabrication can be divided into three categories: natural polymers, synthetic polymers and bioceramics [17].

Natural polymers are macromolecular substances that could be obtained from animal or plant sources. The representatives include collagen (a collagenous scaffold and its morphology are shown in *Figure 5*), gelatine, glycosaminoglycans (GAGs), chitosan or alginate. The advantage of some natural polymers dwells in the cell binding sites which are present and do not have to be added artificially as in the case of synthetic polymers. The most notable synthetic polymers are polyesters, namely polylactic acid (PLA), polyglycolic acid (PGA) and their copolymer poly-DL-lactic-co-glycolic acid (PLGA). Scaffolds can be also prepared as hydrogels which are considered a subcategory of synthetic polymers and could be fabricated from polyethylene glycol (PEG), polyvinyl alcohol (PVAl) or polyacrylic acid (PAA). Hydrogels are made by crosslinking water-soluble polymers resulting in a formation of an insoluble network that is then coated with an adhesive protein to create binding sites for cells. The last group of biomaterials, bioceramics, is common in bone tissue engineering (BTE) and comprises three primarily used compounds: Hydroxyapatite (HAp), which exists in human body as a bone mineral, and α and β modifications of tricalcium phosphate (α-TCP and β-TCP). These non-metallic crystalline compounds are biocompatible, osteoconductive and have different solubility in aqueous environment. The different solubilities of these three minerals are mainly utilized in the preparation of suitable carriers for BTE [5, 17].

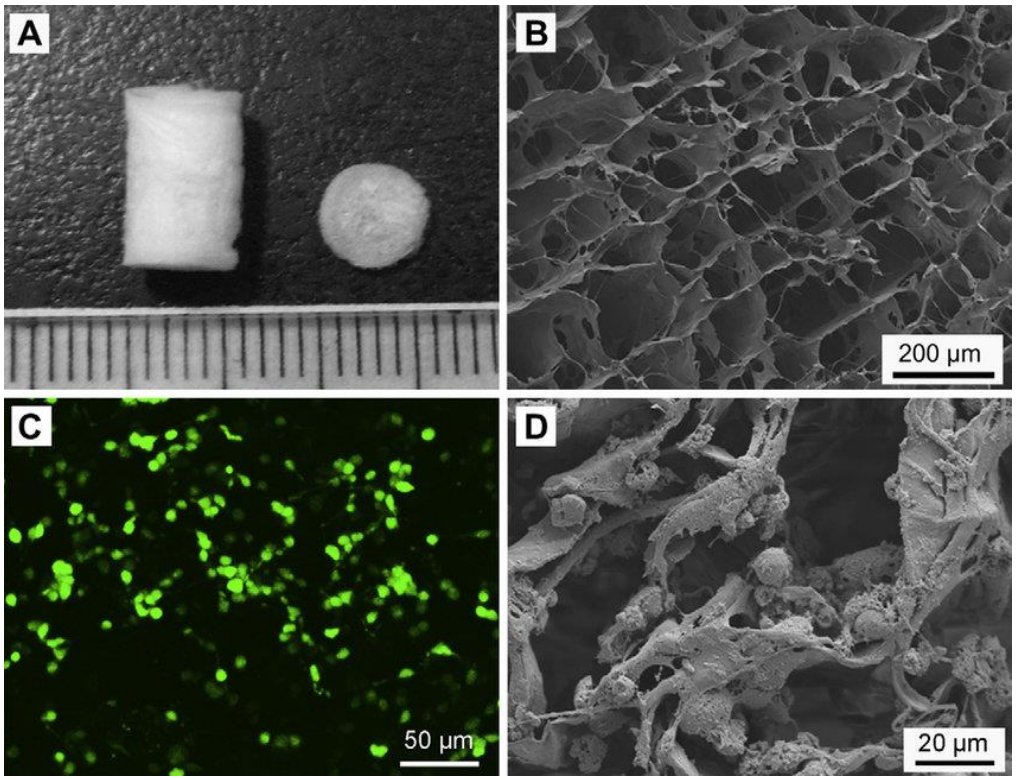

Figure 5 – (A) Porous collagen scaffold as seen by a normal eye. (B) Morphology of the scaffold depicted by SEM image. (C) Confocal image of Fluorescein diacetate (FDA) staining and (D) SEM image, both of the scaffold seeded with neural progenitor cells (NPCs) after 7 days of culturing [19].

2.3.1 Scaffold Fabrication by Freeze-drying

Nowadays, freeze-drying is the most frequently used technique for 3D scaffold fabrication in tissue engineering. Freeze-drying (FD) is a method which uses sublimation of a frozen phase to dispose of the solvent. Its extensive use in TE comes from the fact it works in lower temperatures and does not apply heat impactfully. This suits heat sensitive compounds like natural polymers to retain their biological properties after processing. FD avoids evaporation curve in the phase diagram of the solvent, utilizing the freezing and sublimation (drying) processes. This also helps to retain the pore morphology in a scaffold where the structure could be disrupted by the vapour pressure, making it less uniform.

Scaffolds created by FD can achieve porosity surpassing 90 % and pore size in the range between 20 and 400 µm, making them suitable for use in skin and bone tissue engineering. The properties of the resulting scaffolds are tailored through freeze-drying settings (e.g. temperature decrease rate, pressure of the chamber) and solution parameters (e.g. viscosity, polymer concentration, type of the solvent and polymer) [20].

2.4 Scaffold Materials

2.4.1 Collagen

Collagen is the human body's most abundant protein as it forms 30 to 35 % of its total protein mass. Collagen occurs in every connective tissue and its fibrillar form is a major constituent of

the ECM, where it provides cells with structural and mechanical support while also regulating their biological functions when they adhere to its surface [22, 23].

Structurally, collagen is composed out of collagenous and non-collagenous domains. The primary structure of collagenous domains are repeating peptide triplets consisting of the amino acid template Gly-X-Y [22]. The X and Y positions are most often occupied by proline and its hydroxylated form 4-hydroxyproline [23, 24]. Domains of this composition then fold into left-handed α-helix with 18 amino acids per turn, able to expose their glycine residues towards a fixed axis. The 4-hydroxyproline residues are crucial for this secondary structural motif as they form intramolecular hydrogen bonds, thermally stabilising the structure. Three of these α-chains conjoin around a central axis into supramolecular structure called triple helix [24]. The triple helix is a right-handed coil where the glycine residues of all three molecules are closely packed together across the axis [23]. Non-collagenous domains differ from the collagenous in the amino acid sequence. They do not follow the Gly-X-Y template and therefore even their spatial organisation is diverging from the collagenous. If it were not for their existence, all collagen in the human body would be fibrillar. The structure and functions of these domains are diverse and their combination with collagenous domains in varying manners leads to the existence of 30 currently known collagen types [24].

Collagen types are marked with Roman numerals from I to XXX according to occurrence frequency and order of their discovery [25]. They are divided into various separate families that correspond with their structure and function. Collagens can be categorised as fibril-forming, Fibril-associated collagens with interrupted triple helices (FACITs), FACIT-like collagens, network-forming, transmembrane, multiple triple-helix domains and interruptions (Multiplexins) or other collagens, that do not fit with the previous groups [25, 26]. The fibril-forming collagens (types I, II, III, V, XI, XXIV, XXVII) are commonly used in tissue engineering for the preparation of 3D scaffolds, because they are the basic building block of the extracellular matrix, which the biopolymer scaffolds desire to imitate. [27].

First steps of the collagen fibre synthesis are taken within the cell walls. At first, a pro-α chain is translated from mRNA in rough endoplasmic reticulum. Afterwards, post-translational modifications, namely hydroxylation of proline and lysine and glycosylation of the hydroxylated lysine, are performed. Modified chain groups up with two more chains and forms a procollagen triple helix with loose ends. Procollagen is transported into the Golgi apparatus, encapsulated into excretory vesicles and secreted into the extracellular space where the loose ends of procollagen are cleaved, forming tropocollagen. To connect tropocollagens into fibrils, lysine and hydroxylysine residue chains are modified with the enzyme lysyloxidase which enriches them with carbonyl groups. These carbonyls bond covalently with other lysine and hydroxylysine chains of bordering tropocollagens. Crosslinked tropocollagens provide fibrils 10 to 300 nm long which agglomerate to form 0,5 to 3 μm long fibres [23, 24]. Structural hierarchy of fibrillar collagen beginning from pro-α chains is depicted on a tendon in *Figure 6.*

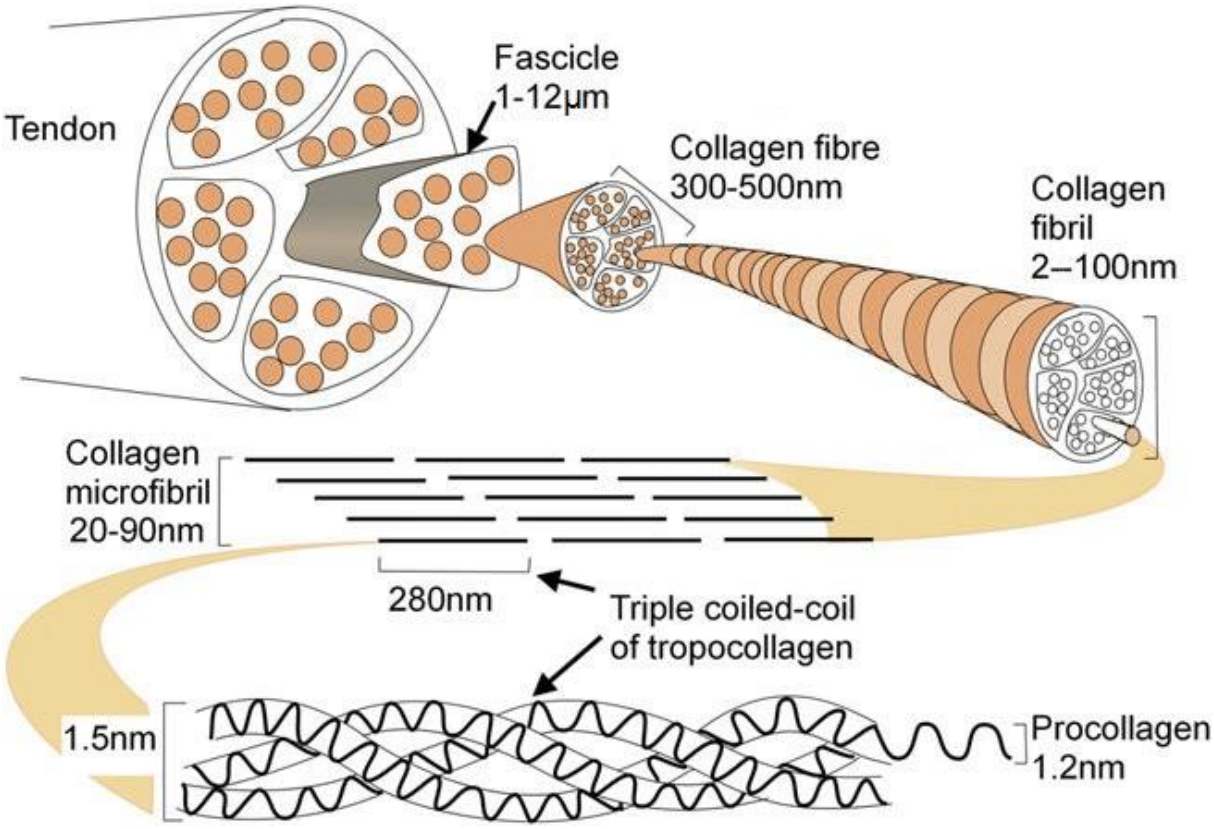

Figure 6 – Hierarchy of collagen ranging from a pro-α chain to a full tendon [28].

Fibrillar collagen does not bear any non-collagenous domains and for this reason its triple helical structure stays uninterrupted [22, 25]. Although some collagen types are more frequent than the other, they do not stay separate and form heterofibrils which are a mixture of two or more fibrillar collagen types. Type I, which appears in skin, bones or tendons and is the most common collagen type, conjoins with types III and V. Type II, that could be found in cornea or cartilage, associates with type XI [25, 27].

Due to the fact collagen is a protein, it is degradable enzymatically. Enzymes used in the degradation process are called collagenases. The whole process begins on the surface, where the first triple helices are damaged and unravelled. This exposes other tropocollagen molecules and allows the enzyme to penetrate further into the fibril. The damaged collagen molecules are vulnerable and can be broken down further by non-specific enzymes which accelerate the degradation process. Crosslinking is used to stabilise the collagen-based scaffolds in tissue engineering as crosslinked substrates endure longer time periods when exposed to collagenase [27, 29].

Crosslinking of collagenous biomaterials can be either physical or chemical. Physical methods, for example UV and gamma irradiation or dehydrothermal treatment, enhance mechanical stability of the scaffold and reduce collagen's water solubility while causing no toxicity issues. Chemical crosslinking provides the stronger covalent bonding but may induce adverse biological response. That is the case of glutaraldehyde which although it creates relatively dense crosslinking, its leftovers pose a toxicity threat. Other important chemical crosslinkers include 1-ethyl-3-(3-dimethylaminopropyl)-carbodiimide hydrochloride (EDC) and N-hydroxysuccinimide (NHS). NHS may or may not be included and is used to

control/slow the reaction rate. EDC mediates the formation of amide between the amine and carboxylic groups in the amino acid side chains but itself it does not enter the newly formed structure, which makes it a so-called zero-length crosslinking agent [29]. Additional possibilities could be seen in using chitosan. Chitosan is a polysaccharide, which, thanks to its amine groups, remains protonated even in acidic solutions and therefore bears a positive electric charge. Collagen is drawn to the polycationic chitosan because of its negatively charged residues which results in ionic (non-covalent) bonding. Although this chitosan-collagen complex is stable, other crosslinking agents could be incorporated to enhance its properties. However, the main advantage of this connection is the fact that chitosan does not induce immunogenic response [29, 30].

Type I collagen became common in tissue engineering, as it is the most easily extractable type. The sources of collagen in TE are mostly from bovine, porcine, sheep and rat species. It is isolated from collagen-rich tissues such as dermis, tendon or bone. While tendons from rat tails, bovine Achilles tendons or its skin are already used for collagen solutions, fish collagen came into spotlight in recent years for its easy extraction and purification from fish skin and bones. The problem with xenogeneic collagen dwells in antigenicity and immunogenicity because certain sequences in the molecule can induce immune response and synthesis of more antibodies. This effect can be suppressed by removing these sequences by pepsin or by cross-linking which shields or modifies them [27, 29, 31].

A large portion of collagen is water insoluble. To extract collagen into a solvent, solution of a neutral salt or dilute acetic acid are used. A strong base or an enzyme employment then helps to break the crosslinking even more [29]. The mechanical load collagen fibres can take is dependent on their structural parameters. The main ones are the diameter and orientation of the fibres. Thick fibres in tendon withstand higher stresses than thinner fibres in lungs. Also, fibres oriented more unidirectionally can bear more load in their direction. Collagen's thermal stability depends on its organization level. Denaturation temperature increases with the hydroxyproline residue content (which provides hydrogen bonding) and with the density of crosslinking. However, water soluble collagen in fully hydrated state denatures around the body temperature of mammals which has to be kept in mind when preparing collagenous scaffolds and selecting fabrication methods [32].

Scaffolds made purely out of collagen, even though they have remarkable biological properties (biocompatibility, biodegradability as well as regulation of cell migration, adhesion and differentiation to name a few), do not suffice in their mechanical strength, especially in the hydrated state. Mechanical and structural properties can be enhanced by crosslinking or preparing composite scaffolds. Blending collagen with natural polymers is one possibility, because the biocompatibility does not differ much from the pure collagen and the mechanical properties increase. Examples of natural polymers used in TE are chitosan (described earlier), silk fibroin, alginate, GAGs or hyaluronic acid. In composites with synthetic polymers, such as PLA, PGA, PEG, PVAl or PLGA, the surface collagen uses its binding sites to interact with cells while the synthetic polymer ensures structural stability and optimal mechanical support. Synthetic polymers used in TE are bioresorbable and do not release toxic degradation products, although these products could shift the pH balance locally given their acidic nature [29].

2.4.2 Cellulose Derivatives

Cellulose is the most available biopolymeric renewable resource on earth. It can be extracted from woody plants and cotton linters in higher quantities for industrial use or from bacteria as bacterial cellulose with higher purity and more favourable properties in terms of medicinal applications [33]. No matter the source, cellulose in its pure form, even though it is highly hydrophilic, is known for its poor solubility in water and common organic solvents. This comes from its strong intra and intermolecular hydrogen bonding and high crystallinity degree which results in its bad processability. Turning cellulose into a water soluble derivative is a good alternative [34, 35].

Cellulose is a polysaccharide consisting of glucose units linked via β-(1→4) glycosidic bonding. Structurally, cellobiose is declared as elementary repeating unit, because it incorporates the glycosidic bond into the structure. From a more chemical approach, anhydroglucose unit (AGU) fits into the role of repeating unit better, having three hydroxyl groups that can be substituted with polymer-analogue reactions. The hydroxyl groups, two being secondary (C2, C3) and one being primary (C6), are responsible for the insolubility of cellulose which can be eliminated by their substitution. The units at the chain's ends may structurally differ from the AGU, but their selective reaction possibilities (e.g. reductive amination of the reducing end) are inconsequential in the perspective of the macromolecule because the main point of making cellulose derivatives dwells in substituting the hydroxyls [33]. Structural units of cellulose are shown in *Figure 7-A.*

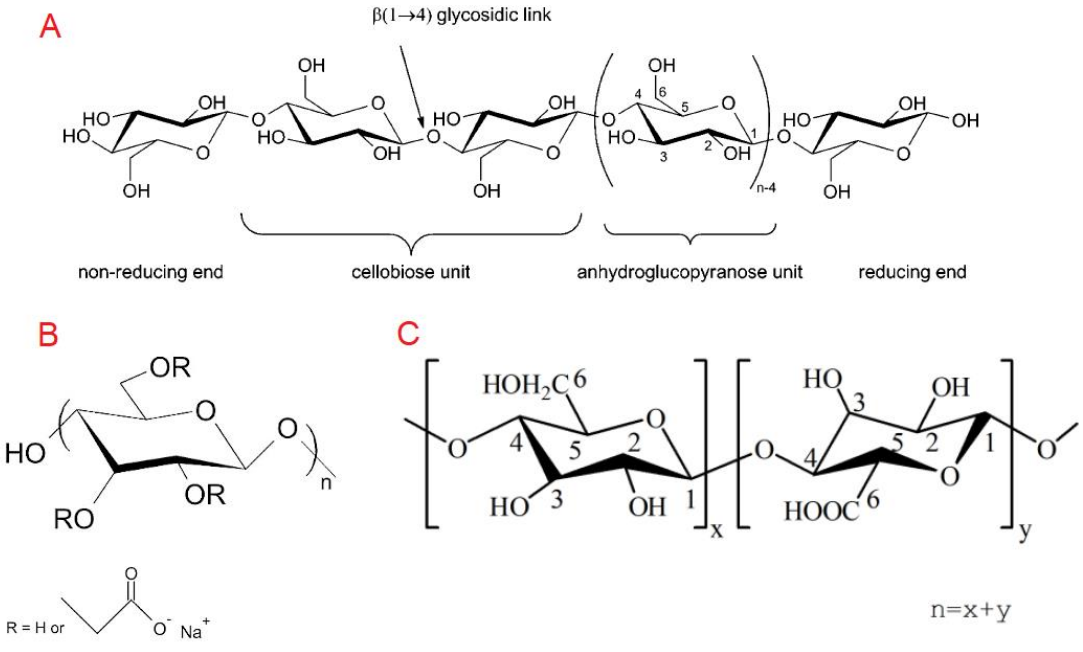

Figure 7 – Structure of cellulose and its derivatives. A – cellulose and its structural units [36]. B – Sodium salt of carboxymethyl cellulose [37]. C – Oxidised cellulose [38].

Prior to derivatisation, cellulose is activated (pre-treated) to access hydroxyl groups hidden within crystalline parts of and achieve homogenous reaction throughout the chain. Most

common pre-treatment is swelling in aqueous solution of alkali. Cellulose derivatives can be organic or inorganic. The major representatives are esters (e.g. cellulose acetate or acetate phthalate) and ethers (e.g. methyl, carboxymethyl or ethyl cellulose) for organic and cellulose nitrate and cellulose sulphate in the inorganic group [33 – 35]. In tissue engineering, for various reasons, there has been an extensive use of carboxymethyl cellulose (*Figure 7-B*) and oxidised cellulose (*Figure 7-C*) which will be the derivatives described further.

2.4.2.1 Carboxymethyl cellulose

In carboxymethyl cellulose (CMC) synthesis, raw cellulose is immersed in aqueous solution of sodium hydroxide to activate it, creating alkali cellulose. The product extracted from the activation step is reacted with monochloroacetic acid or its sodium salt [34]. The hydroxyl groups are generally etherified in C6 > C3 > C2 order and C2 ≈ C6 > C3 order when preparing CMC in heterogenous slurry (activation with a mixture of NaOH and isopropanol). However, full substitution cannot be achieved because of the increasing electrostatic repulsion between the reagent and the chain during the reaction. Degree of substitution (DS) indicates ratio of substituted hydroxyls to AGUs in the chain and affects the properties of the CMC product. CMC needs to be synthesised with DS above 0.4 to be soluble in water. Commercial CMC products have DS in the range of 0.5-1.4. DS can be increased above 1.4 but for that a multi-step reaction is required [33, 39].

CMC finds its extensive use in tissue engineering thanks to its low production costs and excellent biological properties including biodegradability, biocompatibility, non-existent toxicity and insignificant immunogenicity [34]. CMC has polyanionic nature thanks to the carboxyanionic groups which unlock ionic interactions with cations. This can be utilized in combination with bioceramics (HAp, TCPs) where the ion-dipole interaction between COO^- and Ca^{2+} as well as hydrogen bonding between CMC and bioceramics ensure good compatibility This combination is useful for example in composite biodegradable membranes for removal of bisphenol-A from water [39]. CMC combined with collagen can be crosslinked by EDC, creating a bi-molecular template with more reaction sites for binding bioceramics into the matrix, increasing osteoconductivity, osteoinductivity and mechanical strength of the scaffold for bone tissue engineering [40].

2.4.2.2 Oxidised cellulose

Oxidised cellulose (OC) differs from most of the cellulose derivatives in its structure. It has a carboxy group created by oxidation of the primary hydroxyl on C6. This group cannot be formed on C2 and C3 because secondary hydroxyls can oxidise only into carbonyl groups. It can be synthesised by reaction of swollen cellulose with nitrogen dioxide in tetrachloromethane or other non-polar solvents [33]. Properties of the product depend on whether the substrate is natural, regenerated or bacterial cellulose. Products that contain 3-25 % of oxidised (6-carboxyl) groups are considered biocompatible and bioresorbable in human body [38]. However, this lower degree of substitution results in limited solubility of OC.

Majority of the applications of OC in pure form are used as haemostatic agents thanks to its favourable biological properties, although sometimes its swelling and acidity may cause adverse effects [38]. In tissue engineering OC joins collagen in composite scaffolds to slow down its rather fast degradation and enhance the mechanical properties with retention of the

original biocompatibility and hydrophilicity. Example of potential applications of this composite scaffold could be repair of the peripheral nerve using Schwann cells [41].

2.4.3 Bioceramics

Bioceramic compounds have been applied in tissue engineering for their bone structure mimicking abilities. It is a group of inorganic non-metallic crystalline compounds, often called calcium phosphates and labelled $CaPO_4$ [5, 42]. They are parts of calcified (biomineralized) tissues (bones, teeth) and are desired in TE for their biocompatibility, osteoconductivity (support of cell adhesion, differentiation, proliferation and ECM formation) and osteoinductivity (promoting formation of a new bone using signalling and progenitor cell recruitment) [43].

The key parameters of bioceramic components in relation with their properties are the ionic Ca/P molar ratio, acidity/basicity and solubility (particularly in aqueous environment). These three parameters are interconnected as with lower Ca/P ratio the acidity and solubility of $CaPO_4$ increases. Apart from that, calcium phosphates could be characterized by their crystallinity, phase composition or shape of particles [42].

In bone tissue engineering, bioceramics are used in combination with collagen to form hybrid organic/inorganic scaffolds for bone repair. The three main bioceramic substrates are α and β-tricalcium phosphates and hydroxyapatite. Various possibilities have been explored in bone TE such as deposition of HAp onto and throughout freeze-dried collagenous scaffolds in simulated body fluid. This technique ensured surface bonding on the phase interface between the bone and the graft and by that fixation of the graft. However, SEM micrographs have shown that the HAp distribution was not uniform [44]. Other study has shown on collagen/HAp composite, that it is possible to control porosity without changing the composition of the mixture by using air-drying in combination with freeze-drying [45]. Elsewhere, collagen/HAp/β-TCP scaffolds fabricated by cold isostatic method displayed close attachment and Ca^{2+} ion diffusion between the artificial substrate and newly formed bone [46]. A study focusing on freeze-dried collagen/α-TCP/β-TCP scaffolds has proven that by altering the α-TCP/β-TCP ratio it is possible to control porosity, compressive modulus and other properties [47]. These three bioceramic compounds show great promise for the development of bone tissue engineering and for that reason they will be further described.

2.4.3.1 Hydroxyapatite

Hydroxyapatite (HAp), on a structural level, greatly differs from TCPs with its crystalline unit ($Ca_{10}(PO_4)_6(OH)_2$), which consists of two molecules. Its Ca/P ratio of 1.67 indicates worse solubility and greater basicity compared to TCPs. In fact, it is the second least soluble and most stable calcium phosphate after fluorapatite. Consequently, its insolubility opens a possibility of its preparation by precipitation from aqueous solutions. Techniques for HAp creation are either reactions in solid state or wet methods (such as hydrolysis of other $CaPO_4$ or hydrothermal synthesis). It is deemed to be osteoconductive but not osteoinductive, which could be solved by ion substitutions (for example carbonate for phosphate) [42, 48].

HAp is the main inorganic part of biological bone and for that reason it has been the most researched bioceramic compound. Though collagen and HAp alone are not outstanding in terms of mechanical properties, their structural arrangement (*Figure 4*) in bone makes it mechanically

strong nanocomposite. HAp also helps to deal with ion deficiency in body fluids as a source of calcium and phosphorus when resorbed by osteoclasts. However, biological HAp is not pure because it is often calcium deficient (CDHAp) and involves various other cations (Na, Mg, K, Sr) as substitutes of Ca. That said, artificial HAp still shows high similarity to the inorganic bone phase, hence its frequent use in TE [50].

2.4.3.2 β-tricalcium phosphate

β-tricalcium phosphate (β-$Ca_3(PO_4)_2$), shortened as β-TCP, does not appear in calcified tissues unless it is in an ion-substituted form β-tricalcium magnesium phosphate (β-TCMP). It could be prepared by thermal decomposition of CDHAp (calcium-deficient hydroxyapatite) above 800 °C or by precipitation in ethylene glycol at roughly 150 °C. It cannot be precipitated from aqueous solutions because of its partial solubility [42].

Together with hydroxyapatite, β-TCP forms majority of bone grafts, preferably in mix with type I bovine collagen. Though it has remarkable biocompatibility and bio-resorbability its structural stability is poor (partially due to its solubility) [49]. Its mixture with HAp is known as BCP (biphasic calcium phosphate) [43]. Apart from bone grafts, β-TCP together with α-TCP are used in bone cements because of their non-exothermic setting reaction, which creates a possibility of mixing it with temperature-sensitive drugs and other biomolecules [42, 50].

2.4.3.3 α-tricalcium phosphate

α-tricalcium phosphate (α-$Ca_3(PO_4)_2$), shortened as α-TCP is a modification of tricalcium phosphate that forms from β-TCP by phase transfer at 1125 °C. α-TCP is similar to β-TCP in many ways (e.g. same chemical structure, Ca/P ratio) and is prepared by same techniques. The calcination is executed at 1200 °C, however, its preparation is achievable even at lower temperatures than its polymorphic transition (e.g. as silica stabilised α-TCP at 800-1000 °C or by decomposition of low temperature amorphous calcium phosphates at 700 °C).

α-TCP has the same Ca/P ratio as β-TCP (1.5) which would imply it also has the same solubility. However, its crystal structure is different from β-TCP (α-TCP has a less stable crystal lattice). As a result, α-TCP is more soluble and more reactive in aqueous environment [42]. The reactivity enables the possibility of cementic reaction to form CDHAp and harden the bioceramic phase in aqueous conditions [51]. α-TCP is remarkably bioactive and osteoconductive, but it has a disadvantage of its high resorption rate, which exceeds the rate of formation of a new bone. For this reason, it must be employed in biphasic composite as silica stabilized α-TCP with hydroxyapatite, which has been commercialized for bioceramic porous scaffolds [42, 51].

3 MAIN GOALS OF THE WORK

This bachelor's thesis aimed to complete the following objectives:

- To fabricate 3D porous collagenous composite scaffolds for skin and bone tissue engineering,
- To determine the influence of organic (cellulose derivatives) and inorganic (bioceramics) additives on the physical and chemical properties of the composite scaffolds with the analysis of the:
  - Morphology evaluated by scanning electron microscopy – the microstructure, porosity and pore size,
  - Swelling behaviour,
  - Enzymatic degradation *in vitro*,
  - Mechanical properties in wet state – plateau stress and energy absorption efficiency.

4 EXPERIMENTAL PART

4.1 Chemicals

- Collagen type I – bovine skin derived 100% collagen (Collado spol. s r.o., Czech Republic)
- Hydroxyapatite (HAp), calcined at 1000°C for 3 h of mean particle size 130 nm, (Riedel de Haën, Germany)
- α-tricalcium phosphate (α-TCP) of mean particle size 11.01 μm, containing 92 wt% of α-TCP and 8 wt% of HAp, (Premier Biomaterials, Ireland)
- β-tricalcium phosphate (β-TCP) of mean particle size 4.21 μm, containing 89 wt% of β-TCP and 11 wt% of calcium pyrophosphate, (Fluka Chemie GmbH, Switzerland)
- Oxidised cellulose, calcium salt (Synthesia a.s., Czech Republic)
- Carboxymethyl cellulose, sodium salt, $\bar{M}_w$ ca. 250 000 (Acros Organics B.V.B.A., Belgium)
- N-Hydroxysuccinimide (NHS), diluted to obtain 0.01M solution in 98% ethanol (w/w) (Sigma-Aldrich s.r.o., Germany)
- N-(3-Dimethylaminopropyl)-N′-ethylcarbodiimide hydrochloride (EDC), diluted to obtain 0.02M solution in 98% ethanol (w/w) (Sigma-Aldrich s.r.o., Germany)
- Ultrapure water, type I, prepared on Direct-Q® 3UV Water Purification System (Merck spol. s.r.o., Germany)
- Ethanol 98% p.a. (PENTA s.r.o., Czech Republic)
- Sodium phosphate dibasic, for molecular biology, w ≥ 98.5 % (Sigma-Aldrich s.r.o., Germany)
- Collagenase from Clostridium histolyticum for general use, Type I, 0.25-1.0 FALGPA units/mg solid, ≥125 CDU/mg solid (Sigma-Aldrich s.r.o., Germany)
- Sodium chloride (Lach-Ner s.r.o., Czech Republic)
- Potassium chloride (Lach-Ner s.r.o., Czech Republic)
- Potassium dihydrogen phosphate (Lach-Ner s.r.o., Czech Republic)

4.2 Equipment

- Disintegrator – Ultra Turrax T18 digital (IKA®, Germany)
- VACUBOY, vacuum hand operator (INTEGRA Biosciences AG, Switzerland)
- Freeze-dryer – Epsilon 2-10D LSCplus (Martin Christ Gefriertrocknungsanlagen GmbH, Germany)
- Automatic pipette, labopette®, variable, single channel (Hirschmann Laborgeräte GmbH & Co., Germany)
- High-resolution Scanning Electron Microscope FEI VERIOS 460L (Thermo Fisher Scientific Inc., USA)
- RSA-G2 Solids Analyzer (TA Instruments Inc., USA)

4.3 Scaffold fabrication

4.3.1 Fabrication of Collagen/Cellulose Derivatives Scaffolds

3D porous scaffolds were fabricated according to Sloviková *et al.* [52]. At first, pure bovine collagen was sheared and diluted in pre-refrigerated ultrapure water to form a 0.5% aqueous solution of collagen. The collagen solution was transferred into a 48 well-plate freeze-dried.

To prepare samples with cellulose derivatives, the solution of collagen was split between two beakers and corresponding amounts of OC and CMC were added into the beakers. Both mixtures were homogenised by disintegrator and pipetted into the well-plate. The well-plate was then freeze-dried.

4.3.2 Fabrication of Collagen/Cellulose Derivatives Scaffolds with Bioceramics

The samples for bone tissue engineering were made by adding a mixture of bioceramic components (HAp, α-TCP and β-TCP) into the two solutions (collagen + OC; collagen + CMC). The ratio between the bioceramic components was chosen according previous study by Klieštiková [53]. Both mixtures were homogenised with disintegrator, pipetted into a well-plate and freeze-dried.

Overall, 3 well-plates were filled, preparing a total of 144 cylindrical scaffold samples. The samples differed in chemical composition as well as in the height of the samples. 2 well-plates with the average sample height of 5 mm and 1 well-plate with the sample height of 10 mm were prepared. Types of the samples made are shown in *Table 2*, where Coll represents collagen, OC oxidised cellulose, CMC carboxymethyl cellulose and BC bioceramics.

Table 2 – Types of fabricated samples and their composition. Coll represents collagen, OC oxidised cellulose, CMC carboxymethyl cellulose and BC bioceramics.

Sample	Collagen [wt%]	CMC/OC [wt%]	HAp/α-TCp/β-TCP [wt%]
Coll	100	–	–
Coll/OC	50	50/0	–
Coll/CMC	50	0/50	–
Coll/OC/BC	25	25/0	25/22.5/2.5
Coll/CMC/BC	25	0/25	25/22.5/2.5

4.3.3 Crosslinking of the Scaffolds

After the freeze-drying, all the scaffolds were crosslinked by using the crosslinking agent with carbodiimides. The solution of N-(3-Dimethylaminopropyl)-N′-ethylcarbo-diimide hydrochloride (EDC) and N-Hydroxysuccinimide (NHS) in the ratio of 2:1 was prepared in 98% ethanol according to Sloviková *et al.* [52]. The solution was then deployed into the well-plates in a manner it covered the whole scaffold. Ethanol was periodically replenished because of evaporation which could have caused uncovering of the scaffold.

Two hours later, the samples were washed twice in 0.1 $mol \cdot dm^{-3}$ aqueous solution of Na_2HPO_4 and subsequently three times in distilled water. Finally, well-plates were filled with ultrapure water, put into a freezer and freeze-dried for the second time to obtain the scaffolds in their final form.

Out of the total 144 fabricated samples across 5 scaffold types, 3 samples from each type were used for swelling behaviour analysis, other 3 for enzymatic degradation, 8 for the measuring of mechanical properties to ensure representative results and obtain standard deviation values. One scaffold of each type was used for SEM imaging.

4.4 Morphology and Porosity

The structural features of each scaffold were analysed in the scanning electron microscopy (SEM). At first, to prepare the samples for the analysis, each scaffold was put in liquid nitrogen for approximately 5 minutes. This was done to eliminate the scaffold resiliency and facilitate cutting of the scaffold with a razor blade for a more homogenous surface. After cutting each of the samples into slices 2-3 mm of height, they were attached to aluminium pin stubs using a carbon tape (*Figure 8*) in a manner that the surface formed by the cut was sticking upwards. Before the SEM analysis took place, the samples were coated with 20 nm gold layer on Coater Leica EM ACE600 for conductivity. The Images were taken on High-resolution Scanning Electron Microscope FEI VERIOS 460L with accelerating voltage of 5 kV and current of 25 pA.

To determine the pore size and porosity of the scaffolds, images with the 100x magnification and resolution of 500 μm of each sample were used to establish uniform conditions. The measurements were undertaken in the software ImageJ, using the thresholding function for porosity and line measuring in accordance to the resolution for pore size. The minimum of 30 pore diameters were measured in either horizontal of vertical axis.

Figure 8 – A scaffold sample attached to an aluminium pin stub with the carbon tape.

4.5 Swelling Behaviour

The swelling behaviour of scaffold samples was determined by swelling ratio. The measurement was conducted in phosphate-buffered saline (PBS), prepared according to *Cold Spring Harbor Protocols* [54]. Three samples were chosen from each sample type. Prior to the measurements, the samples were weighed in dry state. After that, they were immersed in glass vials with PBS solution (*Figure 9*). The data was obtained by weighing the samples in defined time periods. After 3, 5, 10, 15, 20, 30, 45, 60, 90 and 120 minutes each sample was removed

from the solution, carefully dried with filtration paper to remove physically non-bound water and weighed. The swelling ratio for each time interval was calculated from the data according to Equation (1)

$$S_R = \frac{m_w - m_D}{m_D} , \quad (1)$$

where S_R is swelling ratio, m_w is mass of the wet sample after corresponding time period and m_D is mass of the dry scaffold.

Figure 9 – A scaffold sample before (left) and after (right) immersion in PBS solution in the swelling behaviour and enzymatic degradation analyses.

4.6 Enzymatic Degradation

The enzymatic degradation was realised *in vitro* by a solution of collagenase in PBS at 37 °C. Corresponding amount of collagenase from Clostridium histolyticum was dissolved in PBS to obtain a solution with collagenase concentration of 2,2 mg·dm^{-3}. The solution was then tempered at 37 °C for 1 hour. Scaffold samples were immersed in PBS for 30 minutes (according to the swelling behaviour results) at 37 °C, deprived of the excess water and weighed in wet state. Afterwards, the PBS solution in the glass vials was replaced by the collagenase solution. Samples were inserted into the vials and put into incubator (37 °C) to simulate the physiological conditions. Each sample was removed from the solution, dried with filtration paper and weighed in the 1, 2, 4, 8, 24, 48 and 72 h intervals from the first immersion. To calculate the mass loss of each sample, the obtained data were put into Equation (2)

$$M_L = \frac{m_i - m_t}{m_i} , \quad (2)$$

where M_L indicates the mass loss, m_i the initial mass of a wet scaffold after PBS swelling and m_t mass of that scaffold after corresponding elapsed time period.

4.7 Mechanical Properties

Dynamic mechanical analysis (DMA) was performed using the RSA-G2 Solid Analyzer. Measurements were conducted in compression mode with samples in wet state immersed in PBS at 37 °C to simulate physiological conditions. Samples with the average height of 10 mm were used. The strain was applied in constant linear rate 0.05 mm·s^{-1} with an axial force of 0.01 N. Upon achieving a strain of 50 %, the measurement was stopped. The requirement for the data were three correlating measurements with exponential-esque strain-stress curve.

For the quantification of mechanical properties according to ISO 13314 standard, plateau stress and energy absorption efficiency were calculated [55]. Plateau stress (σ_{pl}) was determined as an arithmetical mean of stresses corresponding to compressive strains in the range of 20 to 30 %. Energy absorption efficiency was calculated according to Equation (3)

$$W_e = \frac{W}{\sigma_{max} \cdot \varepsilon_{max}} \ , \tag{3}$$

where *We* represents energy absorption efficiency, *W* is energy absorption, calculated as area under the stress-strain curve from 0 to 50 % of compressive strain, ε_{max} and σ_{max} are strain and stress maximums in the same strain range.

5 RESULTS AND DISCUSSION

5.1 Microstructure

The internal architecture of each scaffold, which was revealed on the cut-formed cross-section, was assessed by closer examination of SEM micrographs. The Micrographs of all scaffolds with the magnification of 100x are shown in *Figure 10*.

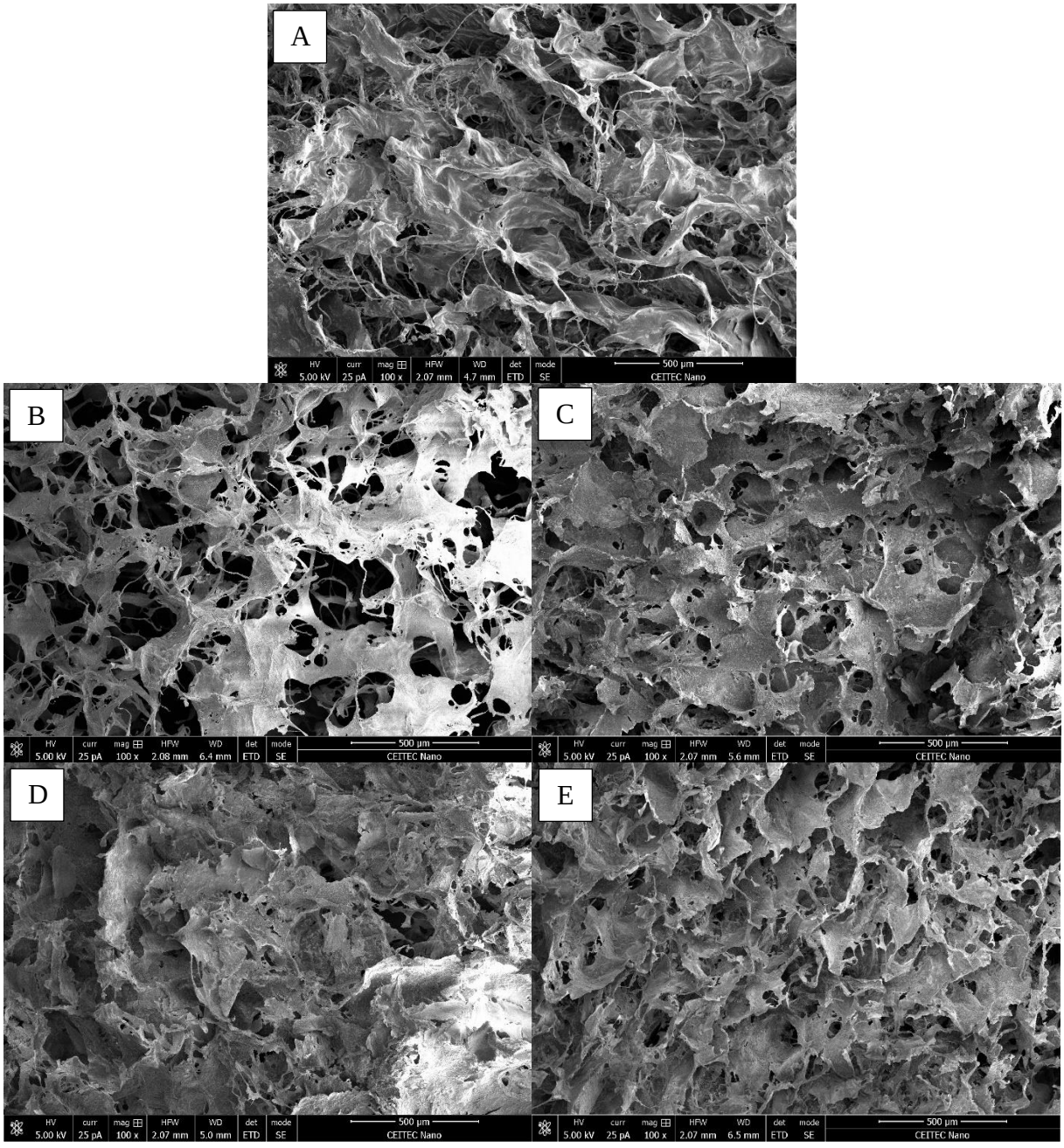

Figure 10 – SEM images of the scaffolds: Coll (A), Coll/OC (B), Coll/CMC (C), Coll/OC/BC (D) and Coll/CMC/BC (E).

A big portion of the purely collagenous scaffold had a fibrous structure, which resulted in bigger pore volume. Fibres were also frequently present in the Coll/OC scaffold and increased its pore size. The proportion of CMC in the Coll/CMC scaffold suppressed the fibrous structure

in its formation and formed plate-like units instead. These plates, present in both types of collagen/cellulose derivative scaffolds, contained circular-shaped cavities that were connecting the neighbouring pores. Both Coll/OC and Coll/CMC scaffolds had a rough surface unlike the pure collagen (Coll) scaffold. This is an important factor for applications in TE as cells adhere better to rougher surfaces.

The addition of bioceramics suppressed the fibre formation even more. The Coll/OC/BC scaffold had more plates than Coll/OC and the plates were also larger in size. The plates grouped closer together than fibres, making the pores smaller. Coll/CMC/BC scaffold achieved the smallest pores and the pores also looked more regular than Coll/CMC scaffold pores. Overall, bioceramics lowered the pore volume and made the scaffold surface even rougher.

The adhesion between the bioceramic particles and biopolymers is important for the functionality of the bone tissue engineering scaffolds. Bioceramics was very well adhered on the surface of both scaffolds, which could be seen in *Figure 11*. Coll/CMC/BC, though, had the bioceramics adhesion and roughness of the surface slightly better. This may be a result of a stronger ionic attraction between bioceramics and CMC, which is more anionic than OC.

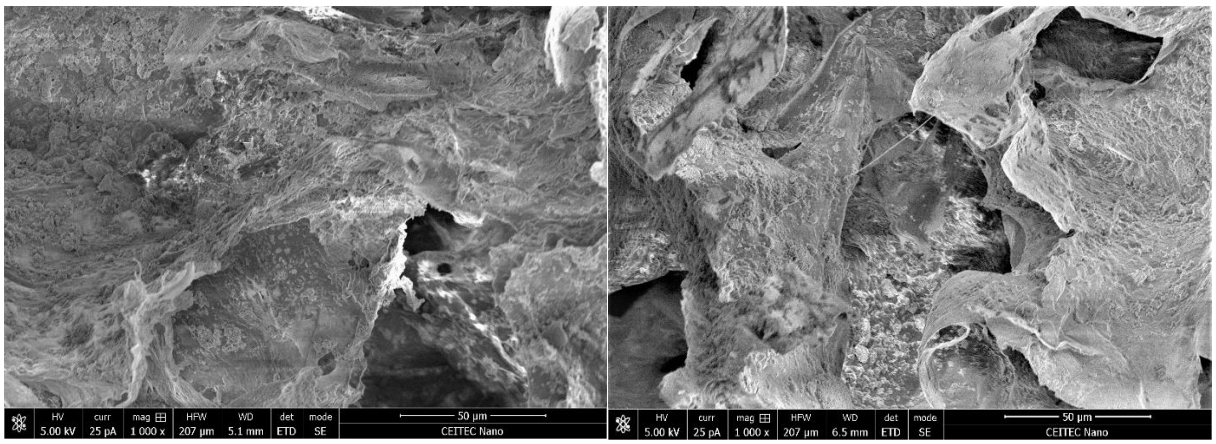

Figure 11 – SEM images of Coll/OC/BC (left) and Coll/CMC/BC scaffolds with a higher magnification to portray the adhesion of bioceramic particles.

5.2 Porosity and Pore Size

Porosity and pore size were determined with the help of the software ImageJ. Both are important parameters of a scaffold, as they affect cell migration, mechanical properties, wet state behaviour and other important factors for the use of scaffolds in TE. Purely collagenous scaffolds achieved the highest porosity with almost 90 % of the structure being the pore network. The collagenous composite scaffolds, however, have reached significantly lower porosity. The collagen composites with cellulose derivatives achieved similar results compared to each other, being only 2 percent apart. Yet the Coll/OC scaffolds which came out more porous than Coll/CMC, have fallen almost 10 % behind the pure collagen scaffolds.

The use of bioceramics lowered the porosity even further. The Coll/OC/BC scaffolds were only 4 % less porous than their non-bioceramic counterparts which is a negligible difference. In the case of CMC containing scaffolds, the difference in porosity was even higher. The

porosity of the Coll/CMC/BC samples was more than 10 % lower than the Coll/CMC combination. This could be the consequence of ionic attraction between positive bioceramics and negative biopolymers which in the case of the last sample resulted in closer clustering, and with that, in lower porosity. The results of the porosity analysis are graphically presented in *Figure 12*.

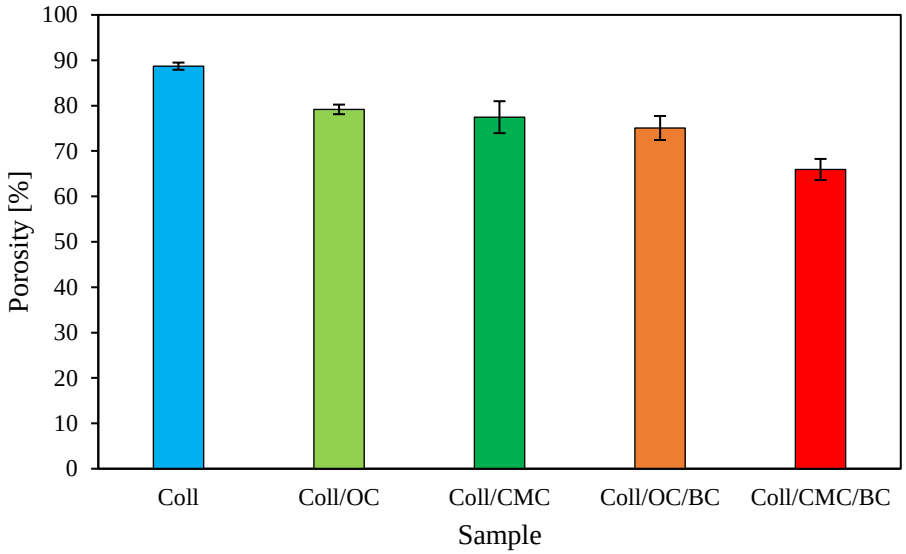

Figure 12 – Porosity of the collagenous and composite scaffolds.

The pore size distribution (shown in *Figure 13*) was quite similar across the different scaffold types. Pore sizes of scaffolds made only out of biopolymers ranged from 100 to 230 μm while the bioceramics addition decreased the lower limit of this range to 80 μm. The widest distribution of pore sizes was noted with samples containing OC which may be due to uneven distribution of the hydrophilic substituted groups in OC.

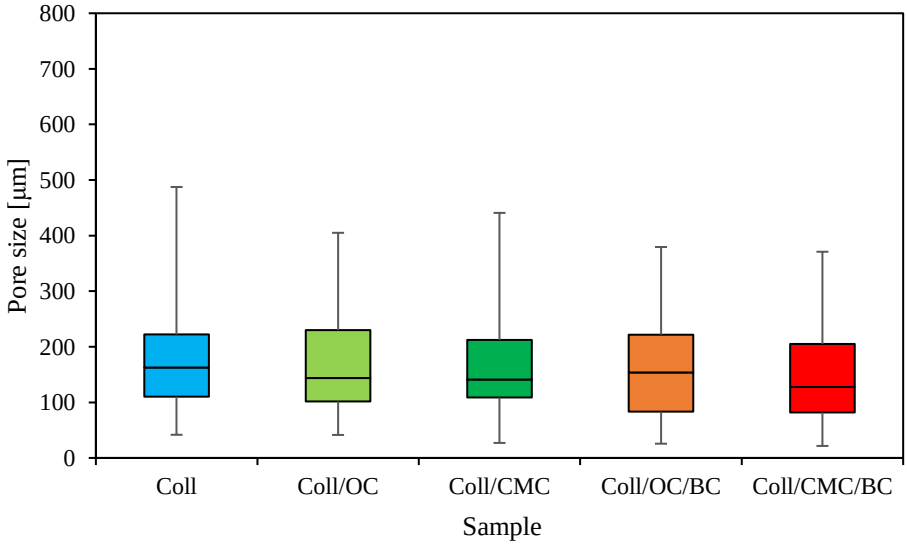

Figure 13 – Pore size distribution displayed from first to third quantile. The line separating the boxes indicates median, the error bars represent minimal and maximal pore size value.

The differences in average size of pores correlated with the differences in porosity as the decreasing trend between the samples appeared similar. The pure collagen samples had the highest average pore size out of all scaffolds, followed by Coll/OC and Coll/CMC samples with results almost identical to each other. Scaffolds with bioceramic particles had the average even lower. Overall, the gaps between the pure Coll, Coll/cellulose derivative, Coll/OC/BC and Coll/OC/BC samples were almost the same. The standard deviation remained between 80 and 100 μm for all samples. Average pore size as well as average porosity of each sample type are displayed in *Table 3*.

The results relate to same conditions in fabrication of each sample. The ideal pore sizes are 20-150 μm for skin scaffolds and 100-500 μm for bone scaffolds (*Table 1*). The average collagen/cellulose derivatives scaffold pores were slightly larger than the ideal pore size for skin scaffolds. The average pores of scaffolds with bioceramics were in the lower values of the ideal bone scaffold pore interval. However, the pore network can be influenced by adjusting the conditions (such as concentration, freeze-drying parameters) to obtain scaffolds with porosity and pore sizes suitable for the desired grafts.

Table 3 – Average porosity and pore size of each scaffold sample.

Sample	Average porosity [%]	Average pore size [μm]
Coll	88.7 ± 0.8	178 ± 99
Coll/OC	79.2 ± 1.1	168 ± 89
Coll/CMC	77.5 ± 3.5	167 ± 99
Coll/OC/BC	75.1 ± 2.6	157 ± 88
Coll/CMC/BC	65.9 ± 2.3	146 ± 82

5.3 Swelling Behaviour

The time dependence of swelling ratio (*Figure 14*) was studied as an indicator of water absorption capacity of each sample. All five data series showed some resemblance. No matter the composition, every sample's swelling ratio peaked between 10 and 30 minutes in the solution. After the peak it remained roughly the same towards the end of the analysis. For that reason, 30 minutes were used in enzymatic degradation as a time limit for swelling samples in PBS prior to weighing them and exposing them to collagenase.

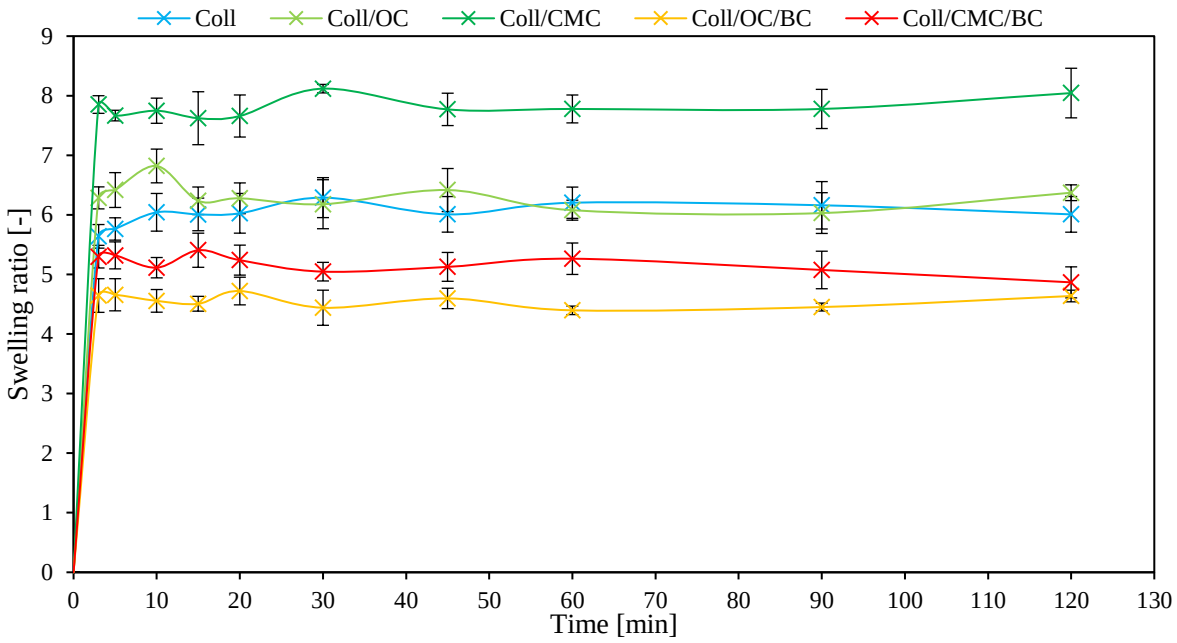

Figure 14 – Swelling Ratio of each type of fabricated scaffolds as a function of time.

Comparing the values individual sample types were ranging in, the scaffolds combining collagen and cellulose derivatives achieved higher swelling ratio than scaffolds containing bioceramics as well. Pure collagen lied in between of these two groups. That is a result of hydrophobicity of bioceramic particles that in addition to water repelling shield the hydrophilic groups of collagen and cellulose they bind to in ionic interactions. Morphology of the scaffolds also contributed to this difference in swelling ratio, as the samples with bioceramics had smaller pore size and lower porosity, both being factors that decreased the water content further.

As for the cellulose derivatives, CMC containing samples showed higher hydrophilicity than those with OC. Apart from the more hydrophilic substituent, CMC also has a higher degree of substitution than OC, resulting in lower content of water-stabilising hydroxyl groups. Moreover, sodium salt of CMC is water-soluble biopolymer while calcium salt of OC is water-insoluble, and therefore, the more hydrophobic cellulose derivative. Comparing to pure collagen, collagen/OC scaffolds had similar results (since both collagen and OC are water-insoluble – just gelling in water) while the swelling ratio of collagen/CMC scaffolds was much higher, due to the explanation above, since CMC is very hydrophilic biopolymer.

5.4 Enzymatic Degradation

The results of enzymatic *in vitro* degradation by collagenase solution in PBS correlated with the results of swelling behaviour to some extent. Samples with cellulose derivatives lost the most of their mass over the course of the degradation while samples containing bioceramics were the least degraded. The pure collagen was in the middle of these two groups. The graphical representation of mass loss of the scaffolds in time is shown in *Figure 15*.

Even though the composite scaffolds contained lesser amount of collagen, which is the subject to degradation, their mass loss was beyond this content. The integrity of the three-dimensional network was severed and as it degraded, smaller pieces of the network were separated from the scaffold. This was confirmed by the visible small chunks present in the

solutions with composite scaffolds. These small pieces of the scaffolds could not be weighed due to their size which consequently lead to increased mass loss. No chunks were observed in the solution with pure collagen scaffolds so even if they may have been released, they have been eventually fully degraded. To sum this up, cellulose derivatives and bioceramic particles were also parts of the mass loss.

The hydrophilicity also influenced the degradation process. Scaffolds which contained CMC ended slightly more degraded than those with OC, which is less hydrophilic. Bioceramics, with its hydrophobic nature, repelled the solution which slowed the degradation. The samples with bioceramics also made their degradation more difficult due to lower porosity and smaller size of pores. Towards the end of the experiment, the mass loss of samples Coll/OC/BC and Coll/CMC/BC was increasing almost insignificantly, indicating complete decomposition of the degradable collagenous part of the scaffolds.

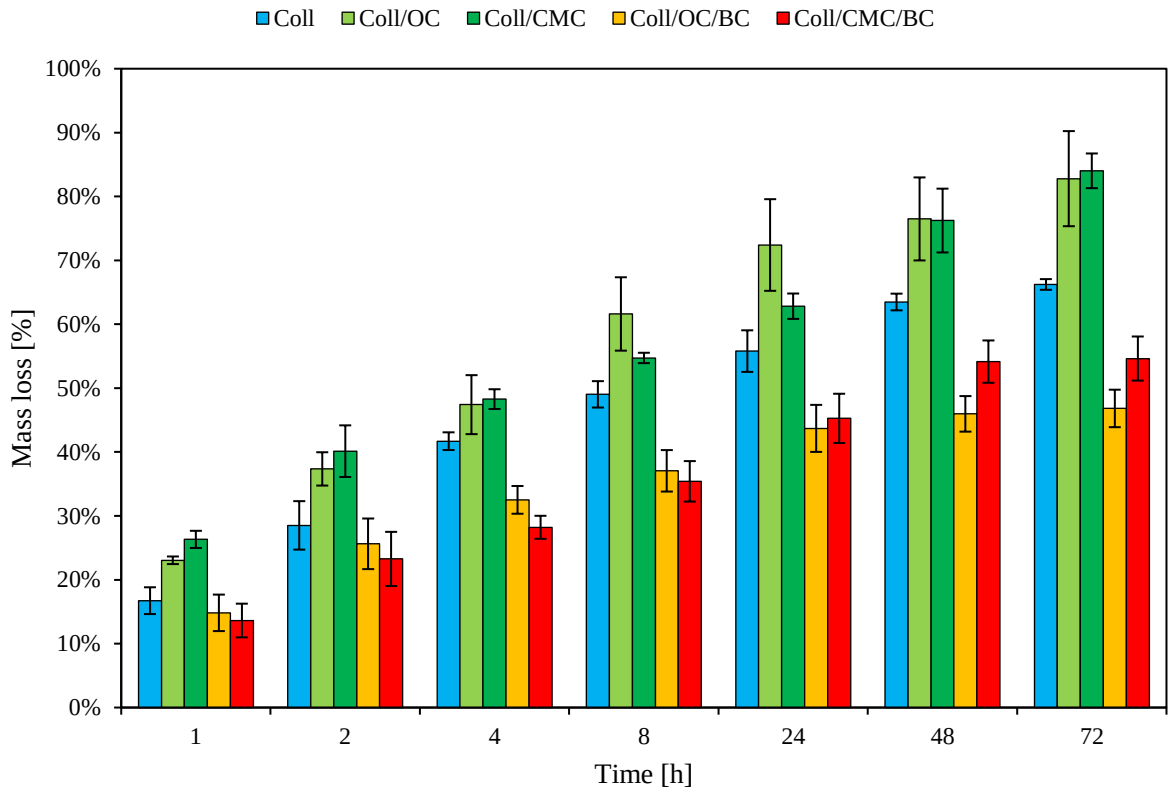

Figure 15 – Mass loss of collagenous and composite scaffolds during the process of enzymatic degradation in PBS solution of collagenase.

5.5 Mechanical Properties

The mechanical properties were determined by dynamic mechanical analysis in wet state, simulating the physiological conditions by PBS tempered to 37 °C. Plateau (yield) stress, which represents the compressive strength of the scaffold is presented for each sample in *Figure 16*. The results are connected to chemical character of the scaffolds (especially to hydrophilicity) and pore morphology.

For the samples without bioceramics, the plateau stress increased with decreasing hydrophilicity. The pure collagen recorded the highest plateau stress out of the three, followed by Coll/OC and the most hydrophilic sample Coll/CMC which achieved the lowest result. The results, however, were not differing that much. This could be explained by the morphology of the pores. Higher porosity and pore size result in lower mechanical stability, which also applies to compressive strength. Pure collagen may be the least hydrophilic out of the non-bioceramic scaffolds, but with the highest porosity and mean pore size out of all samples it does not eclipse the rest by much with its plateau stress values.

Scaffolds with bioceramic particles exceeded the compressive strength of the purely biopolymeric scaffolds by an evident margin. The hydrophobic bioceramic particles repelled the solution from the internal microstructure, resulting in binding lesser amounts of water and greater shape stability in aqueous environment. However, Coll/OC/BC scaffolds, which were the most hydrophobic according to swelling behaviour results, did not achieve the highest plateau stress. They had 32 % higher value than Coll and 43 % higher value than the non-bioceramic Coll/OC, which is a notable difference. Nevertheless, Coll/CMC/BC samples were superior as they achieved plateau stress twice as higher as the pure collagen scaffolds and 139 % higher than the Coll/CMC scaffolds. This was caused by the scaffold pore characteristics. The porosity of the Coll/CMC/BC scaffolds was the lowest out of all scaffold types and significantly lower than the porosity of Coll/OC/BC scaffolds. The low porosity as well as smaller pore sizes provided better structural support for the scaffolds, resulting in higher compressive strength.

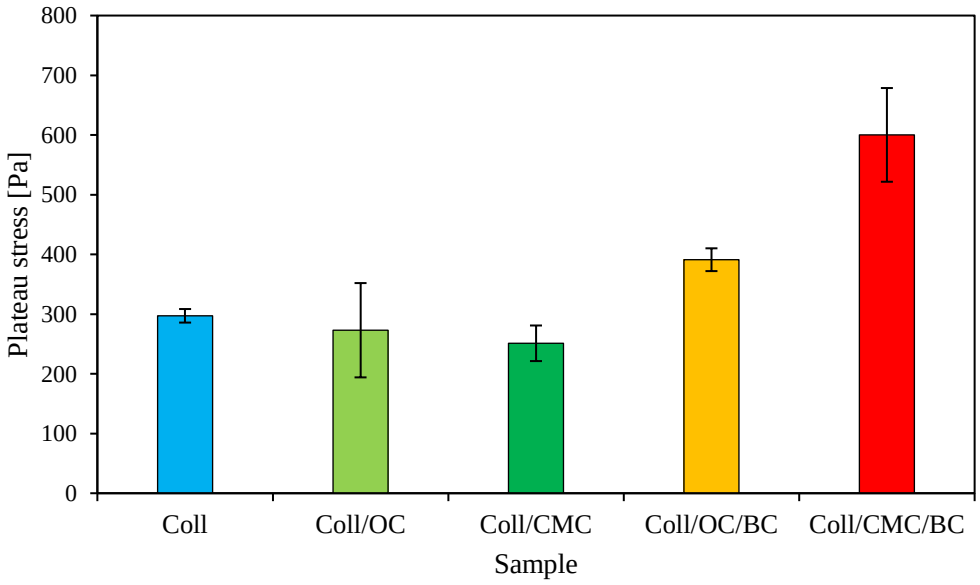

Figure 16 – Plateau stress of all scaffold types.

Another studied parameter in terms of mechanical properties is the energy absorption efficiency which indicates the ability of the sample to absorb deformation energy [53]. All samples achieved similar results except for sample Coll/CMC with energy absorption efficiency slightly lower than the rest. Coll and Coll/OC had the best results which differed from each other only by less than 0.5 %. Scaffolds with bioceramics ended in the middle between Coll/OC and Coll/CMC. Despite the fact Coll/CMC sample ended up as the worst one, the results are still

satisfying in comparison with the rest of the samples. The energy absorption efficiency of each sample is illustrated in *Figure 17*. The exact values of plateau stress and energy absorption efficiency are presented in *Table 4*.

Table 4 – Plateau stress and energy absorption efficiency of each scaffold type.

Sample	σ_{pl} [Pa]	W_e [%]
Coll	297 ± 11	47.8 ± 1.2
Coll/OC	273 ± 79	47.3 ± 4.2
Coll/CMC	251 ± 30	41.4 ± 5.2
Coll/OC/BC	391 ± 19	44.4 ± 7.3
Coll/CMC/BC	600 ± 78	45.4 ± 4.3

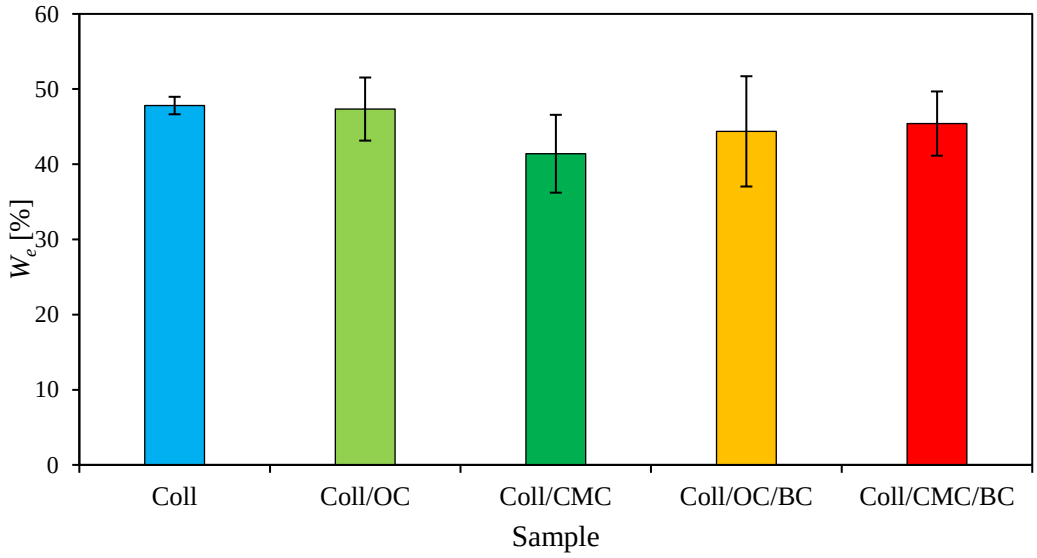

Figure 17 – Energy absorption efficiency of collagenous and composite scaffolds.

6 CONCLUSION

The 3D collagenous composite scaffolds and one type of the pure collagen scaffolds were prepared by using a freeze-drying fabrication method. The scaffolds for possible skin applications were made as combinations of collagen with either oxidised cellulose (Coll/OC) or carboxymethyl cellulose (Coll/CMC). The new scaffolds for possible bone applications were made by adding bioceramics making the Coll/OC/BC and Coll/CMC/BC samples. Purely collagenous scaffolds (Coll) served as a reference.

The morphology was evaluated from SEM images of the scaffold cross-sections. The microstructure showed that the scaffolds with bioceramics and the Coll/CMC scaffold suppressed formation of fibres, which were present in the reference Coll sample and partially in the Coll/OC sample. Instead of the fibres, plate-like structures were formed. The most of these plates were created in the Coll/OC/BC and Coll/CMC/BC scaffolds due to the bioceramic particles addition and decreased the size of their pores. Unlike Coll, the collagen/cellulose derivatives samples had a rough surface which is favourable for cell adhesion. The surface of samples with bioceramics was even rougher and the bioceramic particles were very well adhered to the biopolymeric surface. The highest porosity was achieved by the Coll sample (88.7 %), followed by the Coll/OC (79.2 %), Coll/CMC (77.5 %) and Coll/OC/BC (75.1 %). The lowest results were achieved by the Coll/CMC/BC scaffold (65.9 %). The mean pore size correlated with the porosity results and was between 140 and 180 μm for all samples, which is in the upper limit of ideal pore size for skin scaffolds (20-150 μm) and within the lower limit of ideal pore size for bone scaffolds (100-500 μm). The distribution of pore sizes was similar across all scaffolds. With the addition of bioceramics, however, the lower limit of the pore size range decreased by approximately 20 μm.

The results of swelling behaviour analysis indicated hydrophilicity and the crosslinking conversion of the samples. Samples with CMC had higher swelling ratio than their counterparts with OC due to their more hydrophilic nature that comes from a higher degree of substitution and more hydrophilic substituent. As a result, Coll/CMC/BC samples were more hydrophilic due to the CMC water solubility compared to Coll/OC/BC, where OC is water insoluble. The collagen/cellulose derivatives samples were the most hydrophilic while the samples with addition of bioceramics were the most hydrophobic. The pure collagen scaffolds lied in the middle of the two groups. Bioceramics decreased the hydrophilicity because it repelled the water from the internal microstructure and blocked the hydrophilic groups of biopolymers. Samples with bioceramics also had lower porosity and smaller pores, which decreased their water content further.

The results of the enzymatic degradation *in vitro* correlated with the results of swelling behaviour. By repelling the solution due to its hydrophobic character, the bioceramics slowed the degradation process. The most hydrophilic samples Coll/OC and Coll/CMC ended as the most degraded after 72 hours of immersion in collagenase PBS solution, while the least hydrophilic samples Coll/OC/BC and Coll/CMC/BC had the lowest mass loss. The collagen sample ended in the middle, similarly as in the swelling analysis. The structure of the composite scaffolds was severed in the process and smaller chunks were separated from the surface of the scaffolds. This resulted in a bigger mass loss than the collagen content of those scaffolds.

Plateau stress and energy absorption efficiency were obtained from dynamic mechanical analysis in wet state. Highest compressive strength, presented by the plateau stress, was achieved by the Coll/CMC/BC sample with 600 Pa (139 % higher than Coll/CMC), followed by the second bioceramic composite scaffold Coll/OC/BC with 391 Pa (43 % higher than Coll/OC). The collagen/cellulose derivatives scaffolds Coll/OC with 273 Pa and Coll/CMC with 251 Pa had significantly lower compressive strength than the samples with bioceramics and even lower than the collagen reference with 297 Pa. The increase of compressive strength by the addition of bioceramics was the highest in the samples with CMC. The compressive strength increased with decreasing hydrophilicity and porosity. The Coll/CMC/BC scaffolds resulted the best, even though they were the second least hydrophilic. These scaffolds had the lowest porosity out of all samples by a big difference and the low porosity acted as a support to their structure in compression. Energy absorption efficiency (*We*) represented the scaffold's ability to absorb deformation energy. Coll (47.8 %) and Coll/OC (47.3 %) had the highest *We*, followed by the scaffolds with bioceramics Coll/CMC/BC (45.4 %) and Coll/OC/BC (44.4 %). Coll/CMC (41.4 %) scaffolds were the least efficient in absorbing the deformation energy. However, the results of energy absorption efficiency compared to each other were almost similar.

7 REFERENCES

[1] LANGER, R a J. VACANTI. Tissue engineering. *Science* [online]. 1993, **260**(5110), 920-926 [cit. 2020-02-01]. DOI: 10.1126/science.8493529. ISSN 0036-8075. Dostupné z: http://www.sciencemag.org/cgi/doi/10.1126/science.8493529

[2] MACARTHUR, Ben D. a Richard O. C. OREFFO. Bridging the gap. *Nature* [online]. 2005, **433**(7021), 19-19 [cit. 2020-02-01]. DOI: 10.1038/433019a. ISSN 0028-0836. Dostupné z: http://www.nature.com/articles/433019a

[3] KHADEMHOSSEINI, Ali a Robert LANGER. A decade of progress in tissue engineering. *Nature Protocols* [online]. 2016, **11**(10), 1775-1781 [cit. 2020-02-01]. DOI: 10.1038/nprot.2016.123. ISSN 1754-2189. Dostupné z: http://www.nature.com/articles/nprot.2016.123

[4] CHEN, Fa-Ming a Xiaohua LIU. Advancing biomaterials of human origin for tissue engineering. *Progress in Polymer Science* [online]. 2016, **53**, 86-168 [cit. 2020-02-01]. DOI: 10.1016/j.progpolymsci.2015.02.004. ISSN 00796700. Dostupné z: https://linkinghub.elsevier.com/retrieve/pii/S0079670015000386

[5] MURPHY, CM, FJ O'BRIEN, DG LITTLE a A SCHINDELER. Cell-scaffold interactions in the bone tissue engineering triad. *European Cells and Materials* [online]. 2013, **26**, 120-132 [cit. 2020-02-02]. DOI: 10.22203/eCM.v026a09. Dostupné z: http://ecmjournal.org/journal/papers/vol026/pdf/v026a09.pdf

[6] HAY, Elizabeth D. *Cell Biology of Extracellular Matrix: Second Edition* [online]. 2nd ed. New York: Springer US, c1991 [cit. 2020-04-15]. ISBN 978-1-4615-3770-0. Dostupné z: https://books.google.cz/books?id=uwPTBwAAQBA

[7] FRANTZ, C., K. M. STEWART a V. M. WEAVER. The extracellular matrix at a glance. *Journal of Cell Science* [online]. 2010, **123**(24), 4195-4200 [cit. 2020-05-03]. DOI: 10.1242/jcs.023820. ISSN 0021-9533. Dostupné z: http://jcs.biologists.org/cgi/doi/10.1242/jcs.023820

[8] AGHMIUNI, Azadeh Izadyari a Azim Akbarzadeh KHIAVI. Medicinal Plants to Calm and Treat Psoriasis Disease. *Aromatic and Medicinal Plants – Back to Nature* [online]. London: InTech, 2017, 2017-03-15, s. 1-28 [cit. 2020-05-20]. DOI: 10.5772/67062. ISBN 978-953-51-7348-9. Dostupné z: http://www.intechopen.com/books/aromatic-and-medicinal-plants-back-to-nature/medicinal-plants-to-calm-and-treat-psoriasis-disease

[9] STOJIC, Marija, Verónica LÓPEZ, Andrés MONTERO, Cristina QUÍLEZ, Gonzalo DE ARANDA IZUZQUIZA, Lucy VOJTOVA, José LUIS JORCANO a Diego VELASCO. Skin tissue engineering. *Biomaterials for Skin Repair and Regeneration* [online]. Cambridge: Elsevier, 2019, 2019, s. 59-99 [cit. 2020-05-13]. DOI: 10.1016/B978-0-08-102546-8.00003-0. ISBN 978-0-08-102546-8. Dostupné z: https://linkinghub.elsevier.com/retrieve/pii/B9780081025468000030

[10] NG, Keng Wooi a Wing Man LAU. Skin Deep. DRAGICEVIC, Nina a Howard I. MAIBACH. *Percutaneous Penetration Enhancers Chemical Methods in Penetration Enhancement* [online]. Berlin, Heidelberg: Springer Berlin Heidelberg, 2015, s. 3-11 [cit. 2020-05-13]. DOI: 10.1007/978-3-662-45013-0_1. ISBN 978-3-662-45012-3. Dostupné z: http://link.springer.com/10.1007/978-3-662-45013-0_1

[11] BENSON, Heather A. E. a Adam C. WATKINSON, ed. *Topical and Transdermal Drug Delivery: Principles and Practice* [online]. Hoboken, New Jersey: John Wiley, c2012 [cit. 2020-05-14]. ISBN 978-1-118-14049-9. Dostupné z: https://onlinelibrary.wiley.com/doi/book/10.1002/9781118140505

[12] RHO, Jae-Young, Liisa KUHN-SPEARING a Peter ZIOUPOS. Mechanical properties and the hierarchical structure of bone. *Medical Engineering & Physics* [online]. 1998, **20**(2), 92-102 [cit. 2020-05-08]. DOI: 10.1016/S1350-4533(98)00007-1. ISSN 13504533. Dostupné z: https://linkinghub.elsevier.com/retrieve/pii/S1350453398000071
[13] CLARKE, Bart. Normal Bone Anatomy and Physiology. *Clinical Journal of the American Society of Nephrology* [online]. 2008, **3**(Supplement 3), S131-S139 [cit. 2020-05-07]. DOI: 10.2215/CJN.04151206. ISSN 1555-9041. Dostupné z: http://cjasn.asnjournals.org/lookup/doi/10.2215/CJN.04151206
[14] MANOLAGAS, Stavros C. Birth and Death of Bone Cells: Basic Regulatory Mechanisms and Implications for the Pathogenesis and Treatment of Osteoporosis*. *Endocrine Reviews* [online]. 2000, **21**(2), 115-137 [cit. 2020-05-08]. DOI: 10.1210/edrv.21.2.0395. ISSN 0163-769X. Dostupné z: https://academic.oup.com/edrv/article/21/2/115/2423739
[15] WEINER, S. a H. D. WAGNER. THE MATERIAL BONE: Structure-Mechanical Function Relations. *Annual Review of Materials Science* [online]. 1998, **28**(1), 271-298 [cit. 2020-05-07]. DOI: 10.1146/annurev.matsci.28.1.271. ISSN 0084-6600. Dostupné z: http://www.annualreviews.org/doi/10.1146/annurev.matsci.28.1.271
[16] PALMQUIST, Anders. A multiscale analytical approach to evaluate osseointegration. *Journal of Materials Science: Materials in Medicine* [online]. 2018, **29**(5), 1-10 [cit. 2020-05-25]. DOI: 10.1007/s10856-018-6068-y. ISSN 0957-4530. Dostupné z: http://link.springer.com/10.1007/s10856-018-6068-y
[17] GIBSON, Lorna. *Tissue Engineering Scaffolds: Processing and Properties*. In: *Youtube* [online]. Cambridge (Massachusetts): Massachusetts Institute of Technology, 2016 [cit. 2020-06-25]. Dostupné z: https://www.youtube.com/watch?v=Txidu-5VYfU
[18] O'BRIEN, F. Influence of freezing rate on pore structure in freeze-dried collagen-GAG scaffolds. *Biomaterials* [online]. 2004, **25**(6), 1077-1086 [cit. 2020-06-26]. DOI: 10.1016/S0142-9612(03)00630-6. ISSN 01429612. Dostupné z: https://linkinghub.elsevier.com/retrieve/pii/S0142961203006306
[19] LI, Xiaoran, Zhifeng XIAO, Jin HAN, et al. Promotion of neuronal differentiation of neural progenitor cells by using EGFR antibody functionalized collagen scaffolds for spinal cord injury repair. *Biomaterials* [online]. 2013, **34**(21), 5107-5116 [cit. 2020-06-26]. DOI: 10.1016/j.biomaterials.2013.03.062. ISSN 01429612. Dostupné z: https://linkinghub.elsevier.com/retrieve/pii/S0142961213003840
[20] FERESHTEH, Zeinab. Freeze-drying technologies for 3D scaffold engineering. *Functional 3D Tissue Engineering Scaffolds* [online]. Cambridge: Elsevier, 2018, 2018, s. 151-174 [cit. 2020-06-28]. DOI: 10.1016/B978-0-08-100979-6.00007-0. ISBN 9780081009796. Dostupné z: https://linkinghub.elsevier.com/retrieve/pii/B9780081009796000070
[21] KESKINTEPE, Levent a Ali EROGLU. Freeze-Drying of Mammalian Sperm. *Cryopreservation and Freeze-Drying Protocols* [online]. New York, NY: Springer New York, 2015, 2015-11-14, s. 489-497 [cit. 2020-06-28]. Methods in Molecular Biology. DOI: 10.1007/978-1-4939-2193-5_25. ISBN 978-1-4939-2192-8. Dostupné z: http://link.springer.com/10.1007/978-1-4939-2193-5_25
[22] GORDON, Marion K. a Rita A. HAHN. Collagens. *Cell and Tissue Research* [online]. 2010, **339**(1), 247-257 [cit. 2020-07-10]. DOI: 10.1007/s00441-009-0844-4. ISSN 0302-766X. Dostupné z: http://link.springer.com/10.1007/s00441-009-0844-4

[23] PARENTEAU-BAREIL, Rémi, Robert GAUVIN a François BERTHOD. Collagen-Based Biomaterials for Tissue Engineering Applications. *Materials* [online]. 2010, **3**(3), 1863-1887 [cit. 2020-07-10]. DOI: 10.3390/ma3031863. ISSN 1996-1944. Dostupné z: http://www.mdpi.com/1996-1944/3/3/1863

[24] ON DER MARK, KLAUS. Structure, Biosynthesis and Gene Regulation of Collagens in Cartilage and Bone. *Dynamics of Bone and Cartilage Metabolism* [online]. Amsterdam: Elsevier, 2006, 2006, s. 3-40 [cit. 2020-07-10]. DOI: 10.1016/B978-012088562-6/50002-9. ISBN 9780120885626. Dostupné z: https://linkinghub.elsevier.com/retrieve/pii/B9780120885626500029

[25] MIENALTOWSKI, Michael J. a David E. BIRK. Structure, Physiology, and Biochemistry of Collagens. *Progress in Heritable Soft Connective Tissue Diseases* [online]. Dordrecht: Springer Netherlands, 2014, 2014-12-14, s. 5-29 [cit. 2020-07-10]. Advances in Experimental Medicine and Biology. DOI: 10.1007/978-94-007-7893-1_2. ISBN 978-94-007-7892-4. Dostupné z: http://link.springer.com/10.1007/978-94-007-7893-1_2

[26] SORUSHANOVA, Anna, Luis M. DELGADO, Zhuning WU, et al. The Collagen Suprafamily: From Biosynthesis to Advanced Biomaterial Development. *Advanced Materials* [online]. 2019, **31**(1), 1-39 [cit. 2020-07-10]. DOI: 10.1002/adma.201801651. ISSN 09359648. Dostupné z: http://doi.wiley.com/10.1002/adma.201801651

[27] HELARY, Christophe a Abhay PANDIT. Collagen-Based Biomaterials for Regenerative Medicine. *Biomimetic Approaches for Biomaterials Development* [online]. Weinheim, Germany: Wiley, 2012, 2012-12-18, s. 55-74 [cit. 2020-07-10]. DOI: 10.1002/9783527652273.ch3. ISBN 9783527652273. Dostupné z: http://doi.wiley.com/10.1002/9783527652273.ch3

[28] SCARR, Graham. Helical tensegrity as a structural mechanism in human anatomy. *International Journal of Osteopathic Medicine* [online]. 2011, **14**(1), 24-32 [cit. 2020-07-10]. DOI: 10.1016/j.ijosm.2010.10.002. ISSN 17460689. Dostupné z: https://linkinghub.elsevier.com/retrieve/pii/S1746068910001082

[29] DONG, Chanjuan a Yonggang LV. Application of Collagen Scaffold in Tissue Engineering: Recent Advances and New Perspectives. *Polymers* [online]. 2016, **8**(2), 1-20 [cit. 2020-07-10]. DOI: 10.3390/polym8020042. ISSN 2073-4360. Dostupné z: http://www.mdpi.com/2073-4360/8/2/42

[30] MARTÍNEZ, A., M.D. BLANCO, N. DAVIDENKO a R.E. CAMERON. Tailoring chitosan/collagen scaffolds for tissue engineering: Effect of composition and different crosslinking agents on scaffold properties. *Carbohydrate Polymers* [online]. 2015, **132**, 606-619 [cit. 2020-07-10]. DOI: 10.1016/j.carbpol.2015.06.084. ISSN 01448617. Dostupné z: https://linkinghub.elsevier.com/retrieve/pii/S0144861715006025

[31] GORGIEVA, Selestina a Vanja KOKOL. Collagen- vs. Gelatine-Based Biomaterials and Their Biocompatibility: Review and Perspectives. *Biomaterials Applications for Nanomedicine* [online]. London: InTech, 2011, 2011-11-16, s. 17-52 [cit. 2020-07-11]. DOI: 10.5772/24118. ISBN 978-953-307-661-4. Dostupné z: http://www.intechopen.com/books/biomaterials-applications-for-nanomedicine/collagen-vs-gelatine-based-biomaterials-and-their-biocompatibility-review-and-perspectives

[32] MEYER, Michael. Processing of collagen based biomaterials and the resulting materials properties. *BioMedical Engineering OnLine* [online]. 2019, **18**(1), 1-74 [cit. 2020-07-11]. DOI: 10.1186/s12938-019-0647-0. ISSN 1475-925X. Dostupné z: https://biomedical-engineering-online.biomedcentral.com/articles/10.1186/s12938-019-0647-0

[33] HEINZE, Thomas, Omar A. EL SEOUD a Andreas KOSCHELLA. *Cellulose derivatives: synthesis, structure, and properties* [online]. Cham, Switzerland: Springer, [2018] [cit. 2020-07-12]. Springer Series on Polymer and Composite Materials. ISBN 978-3-319-73168-1. Dostupné z: https://link.springer.com/book/10.1007%2F978-3-319-73168-1
[34] OPREA, Madalina a Stefan Ioan VOICU. Recent advances in composites based on cellulose derivatives for biomedical applications. *Carbohydrate Polymers* [online]. 2020, **247**, 1-90 [cit. 2020-07-12]. DOI: 10.1016/j.carbpol.2020.116683. ISSN 01448617. Dostupné z: https://linkinghub.elsevier.com/retrieve/pii/S0144861720308572
[35] CHAVAN, Rahul B, Sneha RATHI, Vaskuri G S Sainaga JYOTHI a Nalini R SHASTRI. Cellulose based polymers in development of amorphous solid dispersions. *Asian Journal of Pharmaceutical Sciences* [online]. 2019, **14**(3), 248-264 [cit. 2020-07-12]. DOI: 10.1016/j.ajps.2018.09.003. ISSN 18180876. Dostupné z: https://linkinghub.elsevier.com/retrieve/pii/S1818087618306603
[36] EYLEY, Samuel a Wim THIELEMANS. Surface modification of cellulose nanocrystals. *Nanoscale* [online]. 2014, **6**(14), 7764-7779 [cit. 2020-07-12]. DOI: 10.1039/C4NR01756K. ISSN 2040-3364. Dostupné z: http://xlink.rsc.org/?DOI=C4NR01756K
[37] CASABURI, Agustina, Úrsula MONTOYA ROJO, Patricia CERRUTTI, Analía VÁZQUEZ a María Laura FORESTI. Carboxymethyl cellulose with tailored degree of substitution obtained from bacterial cellulose. *Food Hydrocolloids* [online]. 2018, **75**, 147-156 [cit. 2020-07-12]. DOI: 10.1016/j.foodhyd.2017.09.002. ISSN 0268005X. Dostupné z: https://linkinghub.elsevier.com/retrieve/pii/S0268005X17307853
[38] ZHANG, Shaohua, Jiwei LI, Shaojuan CHEN, Xiying ZHANG, Jianwei MA a Jinmei HE. Oxidized cellulose-based hemostatic materials. *Carbohydrate Polymers* [online]. 2020, **230**, 1-31 [cit. 2020-07-12]. DOI: 10.1016/j.carbpol.2019.115585. ISSN 01448617. Dostupné z: https://linkinghub.elsevier.com/retrieve/pii/S0144861719312536
[39] HUI, Tao, Shanghuan FENG, Gang CHEN, An LI, Zhongshun YUAN, Hengfu SHUI, Takashi KUBOKI a Chunbao XU. Synthesis of sodium carboxymethyl cellulose using bleached crude cellulose fractionated from cornstalk. *Biomass and Bioenergy* [online]. 2017, **105**, 51-58 [cit. 2020-07-13]. DOI: 10.1016/j.biombioe.2017.06.016. ISSN 09619534. Dostupné z: https://linkinghub.elsevier.com/retrieve/pii/S0961953417302027
[40] HE, Xichan, Keyong TANG, Xiumin LI, Fang WANG, Jie LIU, Fangfang ZOU, Mengyuan YANG a Meixuan LI. A porous collagen-carboxymethyl cellulose/hydroxyapatite composite for bone tissue engineering by bi-molecular template method. *International Journal of Biological Macromolecules* [online]. 2019, **137**, 45-53 [cit. 2020-07-13]. DOI: 10.1016/j.ijbiomac.2019.06.098. ISSN 01418130. Dostupné z: https://linkinghub.elsevier.com/retrieve/pii/S0141813019317490
[41] SONG, Wenli, Yuhua ZHAO, Yadong WU, et al. Fabrication, characterization and biocompatibility of collagen/oxidized regenerated cellulose-Ca composite scaffold for carrying Schwann cells. *International Journal of Biological Macromolecules* [online]. 2018, **119**, 1195-1203 [cit. 2020-07-13]. DOI: 10.1016/j.ijbiomac.2018.08.055. ISSN 01418130. Dostupné z: https://linkinghub.elsevier.com/retrieve/pii/S0141813018324280
[42] DOROZHKIN, Sergei V. *Calcium Orthophosphate-Based Bioceramics and Biocomposites* [online]. Hoboken, New Jersey: Wiley, 2016 [cit. 2020-07-15]. ISBN 9783527699315. Dostupné z: https://onlinelibrary.wiley.com/doi/book/10.1002/9783527699315

[43] BOSE, Susmita, Mangal ROY a Amit BANDYOPADHYAY. Recent advances in bone tissue engineering scaffolds. *Trends in Biotechnology* [online]. 2012, **30**(10), 546-554 [cit. 2020-07-15]. DOI: 10.1016/j.tibtech.2012.07.005. ISSN 01677799. Dostupné z: https://linkinghub.elsevier.com/retrieve/pii/S0167779912001151
[44] LICKORISH, David, John A. M. RAMSHAW, Jerome A. WERKMEISTER, Veronica GLATTAUER a C. Rolfe HOWLETT. Collagen-hydroxyapatite composite prepared by biomimetic process. *Journal of Biomedical Materials Research* [online]. 2004, **68A**(1), 19-27 [cit. 2020-07-15]. DOI: 10.1002/jbm.a.20031. ISSN 0021-9304. Dostupné z: http://doi.wiley.com/10.1002/jbm.a.20031
[45] ANDRONESCU, E., G. VOICU, M. FICAI, I. A. MOHORA, R. TRUSCA a A. FICAI. Collagen/hydroxyapatite composite materials with desired ceramic properties. *Journal of Electron Microscopy* [online]. 2011, **60**(3), 253-259 [cit. 2020-07-15]. DOI: 10.1093/jmicro/dfr010. ISSN 0022-0744. Dostupné z: https://academic.oup.com/jmicro/article-lookup/doi/10.1093/jmicro/dfr010
[46] MATÉ SÁNCHEZ DE VAL, Jose Eduardo, Josè Luis CALVO GUIRADO, Maria Piedad RAMÍREZ FERNÁNDEZ, Rafael Arcesio DELGADO RUIZ, Patricia MAZÓN a Piedad N. DE AZA. In vivo behavior of hydroxyapatite/β-TCP/collagen scaffold in animal model. Histological, histomorphometrical, radiological, and SEM analysis at 15, 30, and 60 days. *Clinical Oral Implants Research* [online]. 2018, **29**(7), 816-816 [cit. 2020-07-15]. DOI: 10.1111/clr.12656. ISSN 09057161. Dostupné z: http://doi.wiley.com/10.1111/clr.12656
[47] ARAHIRA, Takaaki a Mitsugu TODO. Development of novel collagen scaffolds with different bioceramic particles for bone tissue engineering. *Composites Communications* [online]. 2019, **16**, 30-32 [cit. 2020-07-15]. DOI: 10.1016/j.coco.2019.08.012. ISSN 24522139. Dostupné z: https://linkinghub.elsevier.com/retrieve/pii/S2452213919301391
[48] ELIAZ, Noam a Noah METOKI. Calcium Phosphate Bioceramics: A Review of Their History, Structure, Properties, Coating Technologies and Biomedical Applications. *Materials* [online]. 2017, **10**(4) [cit. 2020-07-15]. DOI: 10.3390/ma10040334. ISSN 1996-1944. Dostupné z: http://www.mdpi.com/1996-1944/10/4/334
[49] VADALÀ, Gianluca, Fabrizio RUSSO, Luca AMBROSIO a Vincenzo DENARO. Bioceramics and Biocomposites in Spine Surgery. *Handbook of Bioceramics and Biocomposites* [online]. Cham: Springer International Publishing, 2016, 2016-04-21, s. 967-987 [cit. 2020-07-15]. DOI: 10.1007/978-3-319-12460-5_44. ISBN 978-3-319-12459-9. Dostupné z: http://link.springer.com/10.1007/978-3-319-12460-5_44
[50] GINEBRA, Maria-Pau, Montserrat ESPANOL, Yassine MAAZOUZ, Victor BERGEZ a David PASTORINO. Bioceramics and bone healing. *EFORT Open Reviews* [online]. 2018, **3**(5), 173-183 [cit. 2020-07-15]. DOI: 10.1302/2058-5241.3.170056. ISSN 2396-7544. Dostupné z: https://online.boneandjoint.org.uk/doi/10.1302/2058-5241.3.170056
[51] KIM, Won Jin, Hui-Suk YUN a Geun Hyung KIM. An innovative cell-laden α-TCP/collagen scaffold fabricated using a two-step printing process for potential application in regenerating hard tissues. *Scientific Reports* [online]. 2017, **7**(1) [cit. 2020-07-15]. DOI: 10.1038/s41598-017-03455-9. ISSN 2045-2322. Dostupné z: http://www.nature.com/articles/s41598-017-03455-9
[52] SLOVIKOVÁ, Alexandra, Lucy VOJTOVÁ a Josef JANČAŘ. Preparation and modification of collagen-based porous scaffold for tissue engineering. *Chemical Papers* [online]. 2008, **62**(4) [cit. 2020-07-26]. DOI: 10.2478/s11696-008-0045-8. ISSN 1336-

9075. Dostupné z: http://www.degruyter.com/view/j/chempap.2008.62.issue-4/s11696-008-0045-8/s11696-008-0045-8.xml
[53] KLIEŠTIKOVÁ, N. *Effect of bioceramic additives on morphology, physical and biological properties of collagen scaffolds for bone tissue engineering.* Brno: Brno University of Technology, Faculty of Chemistry, 2018. 86 s. Supervisor of diploma thesis Ing. Jana Brtníková, Ph.D.
[54] Phosphate-buffered saline (PBS). *Cold Spring Harbor Protocols* [online]. 2010, **2006**(1) [cit. 2020-07-16]. DOI: 10.1101/pdb.rec8247. ISSN 1940-3402. Dostupné z: http://www.cshprotocols.org/lookup/doi/10.1101/pdb.rec8247
[55] ISO 13314. *Mechanical testing of metals - Ductility testing - Compression test for porous and cellular metals*. London: IHS, 2011.

8 LIST OF TABLES

9 LIST OF FIGURES

10 LIST OF ABBREVIATIONS

3D	three dimensional
AGU	anhydroglucose unit
BCP	biphasic calcium phosphate
BTE	bone tissue engineering
CaPO4	calcium phosphate
CDHAp	calcium deficient hydroxyapatite
CMC	carboxymethyl cellulose
DS	degree of substitution
ECM	extracellular matrix
EDC	1-ethyl-3-(3-dimethylaminopropyl)-carbodiimide hydrochloride
FACITs	fibril-associated collagens with interrupted triple helices
FD	freeze-drying
FDA	fluorescein diacetate
GAGs	glycosaminoglycans
HAp	hydroxyapatite
NHS	N-hydroxysuccinimide
NPCs	neural progenitor cells
OC	oxidised cellulose
PAA	polyacrylic acid
PBS	phosphate-buffered saline
PEG	polyethylene glycol
PGA	polyglycolic acid
PLA	polylactic acid
PLGA	polylactic-co-glycolic acid
PVAl	polyvinyl alcohol
SEM	Scanning electron microscopy
TE	tissue engineering
UV	ultraviolet
We	energy absorption efficiency
α-TCP	α-tricalcium phosphate
β-TCMP	β-tricalcium magnesium phosphate
β-TCP	β-tricalcium phosphate
σ_{pl}	plateau stress